Palestine Polytechnic University.
College of Engineering and Technology.
Communication and Electronics Engineering.

Flexible Microstrip Antenna for Skin Contact Application.

Project teams:

Amanee Al- Badawi *Asmaa Al- hroub*

Supervisor:
Dr. Osama Ata.

2014-2015

Palestine Polytechnic University

Collage of Engineering

Electrical Engineering Department

Hebron – Palestine

Flexible Microstrip Antenna for Skin Contact Application.

Project Team

Amanee Al- Badawi Asmaa Al- hroub

Submitted to the Collage of Engineering

In partial Electronics and Communication for the degree of

Bachelor degree in Electrical Engineering.

Supervisor Signature

....

Testing Committee Signature

....

Chair of the Department Signature

....

2014-2015

Flexible Microstrip Antenna for Skin Contact Application

A DISSERTATION PRESENTED
BY

AMANEE AL-BADAWI
ASMA HROUB

TO

THE ELECTRICAL ENGINEERING DEPARTMENT

IN PARTIAL FULFILLMENT OF THE REQUIREMENTS
FOR THE DEGREE OF
BACHELOR OF COMMUNICATIONS ENGINEERING
IN THE SUBJECT OF
ANTENNAS

PALESTINE POLYTECHNIC UNIVERSITY
HEBRON, PALESTINE
DECEMBER 2014 - 2015

Abstract

Microstrip antennas are finding a growing medical application in imaging, diagnosis, and treatment. We propose to design and fabricate a flexible microstrip antenna that can be placed in contact with a synthetic skin layer, that has similar electric properties to human breast tumor tissue, as far as dielectric permittivity and impedance are concerned, in order to study the interaction of the antenna with the tissue . The prototype can be considered as the building block of an array for monitoring a breast tumor tissue at a relatively low power level and 2.45 GHz unlicensed frequency, without any requirement of adding a matching medium .

Analytical results, showing the return loss and various radiation pattern with and without the phantom skin, of the designed patch, using High Frequency Simulation Software, Ansoft – HFSS, are presented and discussed. The antenna will be fabricated on a 1.6mm FR4 dielectric layer, covered with very thin copper layers on both sides. The return loss and radiation patterns will be measured in house.

This diagnoses technique promises a competitively easier and safer method than mammography, tomography and other imaging techniques, in which high intensity X-rays for the detection of breast cancer is used .

الملخص

استخدمت هوائيات الميكروسترب في المجال الطبي ، في التصوير والتشخيص والعلاج . تقوم فكرة المشروع على تصميم وتصنيع هوائي الميكروسترب الذي يمكن استخدامه مع طبقة جلد مصنع تحاكي الخصائص الكهربائية لأنسجة الانسان للكشف عن وجود الاورام السرطانية في الثدي دون الحاجة لإضافة الجل الذي يستخدم لعمل الموافقة بين هوائي الميكروسترب والجلد المستخدم . تم تصميم هوائي الميكروسترب ليعمل على تردد ٢.٤٥ جيجا هيرتز، و قياس الفقد الراجع ونمط الاشعاع لهذا الهوائي.

تم محاكاة هذا الهوائي باستخدام برنامج HFSS المحاكي لتصميم الهوائيات على الواقع هذه التقنية في التشخيص اسهل واكثر امنا من تقنيات اخرى مستخدمة في الكشف عن الاورام السرطانية في الثدي مثل الماموغرافي والاشعة السينية التي هي عبارة عن اشعة مؤينة ضارة مع الاستخدام المتكرر.

Contents

Listing of figures

Dedication

This project is lovingly dedicated to our parents and families, thank you for your unconditional support with our studies. We are honored to have you as our families. Thank you for offering us the education we wanted, thank you for giving us a chance to prove and improve ourselves through all our work in this life, for giving all our need during the time we developed our system, and for teaching us that even the largest task can be accomplished if it is done one step at a time. Without your love and support this project would not have been made possible. We would also like to dedicate this project to our friends. Thank you for believing in us, for your unlimited support, everlasting guidance and endless inspiration.

Acknowledgments

First of all, thanks Allah for a lot of merits that led to the successful completion of this project.

We would like to express our gratitude to our supervisor Dr. Osama Ata, Electrical Department, for his continuous supervision . We would like to thank the dean of Palestine Polytechnic University, the chairman of the Electrical Department, as well as the staff of the department. We also would like to thank the staff of the Electrical Department, communication engineering branch especially Eng. Sa'di Tamimi and Mohammad Al-Qaisi. Our families, we would like to present this project for you. Your encouragement made all this possible.

How far you go in life depends on your being tender with the young, compassionate with the aged, sympathetic with the striving and tolerant of the weak and strong. Because someday in life you will have been all of these.

George Washington

1 Introduction

1.1 Historical Background

The concept of microstrip radiators was first proposed by Deschamps in 1953. A patent was issued in France in1955 in the name of Gutton and Baissinot. However, 20 years passed before practical antennas were fabricated. Development during the 1970s was accelerated by the availability of good substrates with low loss tangent and attractive thermal and mechanical properties, improved photolithographic techniques, and better theoretical models. The first practical antennas were developed by Howell and Munson.

Since then, extensive research and development of microstrip antennas and arrays, aimed at exploring their numerous advantages, have led to diversified applications and to the establishment of the topic as a separate entity within the broad field of microwave antennas.[1]

1.1.1 Brief history of breast cancer

Breast cancer has been known to mankind since ancient times. It has been mentioned in almost every period of recorded history. Because of the visible symptoms especially at later stages the lumps that progress to tumors have been recorded by physicians from early times. This is more so because, unlike other internal cancers, breast lumps tend to manifest themselves as visible tumors. Earlier, however, it was a matter of taboo and embarrassment that meant detection and diagnosis was rare. The mention of breast cancers in literature beyond medical journals and books was rare. Involvement of more women and actively bringing out the disease into the open is a recent phenomenon that is around three or four decades old. In the 1990's the symbol of breast cancer - the pink ribbon – brought out a revolution against this cancer. Ancient Egyptians were the first to note the disease more than 3,500 years ago. The condition was described fairly accurately in both Edwin Smith and George Ebers papyri. One of the descriptions refers to bulging tumors of the breast that has no cure. In 460 B.C., Hippocrates, the father of Western Medicine, described breast cancer as a humoral disease. He postulated that the body consisted of four humors - blood, phlegm, yellow bile, and black bile. He suggested that cancer was caused by the excess of black bile. In appearance of the breast cancer too black, hard tumors are seen that burst forth if left untreated to yield a black fluid. He named the cancer karkinos, a Greek word for "crab," because the tumors seemed to have tentacles, like the legs of a crab. Thereafter in A.D. 200, Galen described the cancer as well. He also suggested excessive black bile but, unlike Hippocrates, he postulated that some tumors were more dangerous than others. He suggested medications like opium, castor oil, licorice, sulphur, salves etc. for medicinal therapy of the breast cancers. During this time of history breast cancer was a disease that affected the whole body and thus surgery was not considered. after that progressive research and studies developed in field of breast cancer, new imaging methods were discovered for early breast cancer detection like X-ray, ultrasound, mammography, MRI, each of these methods had side effects beside it's benefit in imaging including used of large quantity of an ionized type of radiation (harmful if repeated many times) , imprecision in diagnoses in many cases and inability to detect small tumors so inability in early diagnoses of breast cancer , in addition the high cost of imaging used these techniques all of these reasons led to research about new imaging methods to overcome all previous side effects.

research in using microstrip antennas had growing up, it used electromagnetic waves in breast cancer imaging , many experiments show the ability of microstrip antennas in imaging breast cancer and early detection using low power of electromagnetic waves which it non ionized type of radiation in contrast of traditional methods mentioned above, in addition to low cost and high ability to detect of small tumors in breast tissues so the ability of early diagnoses to survive large number of patients .[2]

1.1.2 Antennas usage in medical applications

Antennas have long been used in many medical applications including, microwave imaging, medical implants, hyperthermia treatments, and wireless wellness monitoring . Reducing the size and complexity of the antennas used in these applications has been the primary objective of recent antenna research. Many of the above-mentioned medical applications still use bulky antenna systems which impede their efficiency and applicability despite high application potential. Microwave breast imaging can be taken as a very example . The promises of microwave imaging in detecting early breast tumors without using any harmful radiation have drawn considerable attraction in the last decade .[3] However, antennas used in microwave breast imaging devices require to be immersed in intermediate matching [4] liquid medium . The use of such

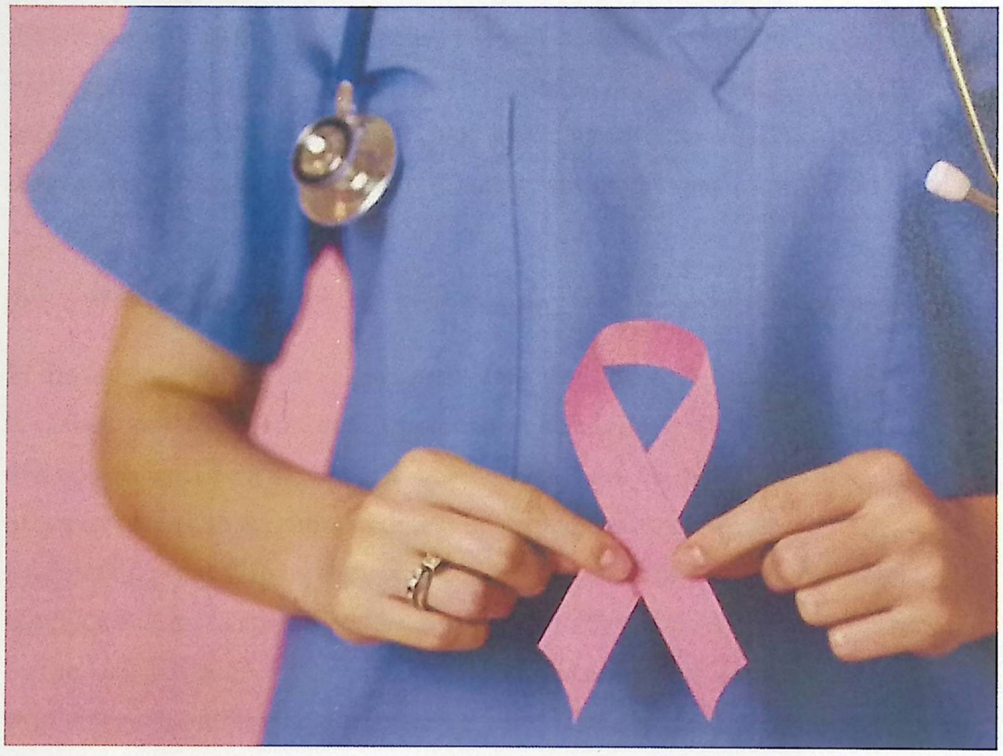

Figure 1.1.1: The symbol of breast cancer - the pink ribbon – brought out a revolution against this cancer.

antennas makes the systems bulky, complicated, impractical, and expensive. The planar and small form factor design of microstrip antennas has attracted growing medical applications . Microstrip antenna design reported for medical applications thus far use nonflexible substrates. We presents a microstrip antenna designed on a non-conventional flexible substrate that can be placed on the skin. The flexibility and the ability to operate in contact with the skin improve the efficiency and practicality while reducing the form factor and cost. For example, the presented antenna in a microwave breast imaging device can remove the need for coupling liquid medium and thus enables the development of wearable breast imaging devices. The design methodology of the antenna, analytical results using simulation models in Ansoft high frequency simulation software (HFSS).[5][6]

1.2 Breast Cancer Screening: Motivation and Goals

In the fight against breast cancer, early detection through screening is the best tool short of a complete cure. Breast cancer screening is defined as the evaluation of a population of asymptomatic women, who have no overt signs or symptoms of breast cancer, in an effort to detect unsuspected disease earlier in its growth" . By detecting cancer in its early stages, it can be identified and treated before it has the opportunity to spread and become potentially lethal. According to a report by the U.S. Institute of Medicine (IOM) in 2001, the ideal screening system would have the following properties: it should be noninvasive, provide minimal discomfort and minimal health risk; furthermore, it should be able to specifically detect malignant tumors at the earliest possible stage, all while being cost effective, easy to perform, and provide conclusive, consistent results. While x-ray mammography currently offers the best combination available of these ideal characteristics, other established imaging techniques, such as ultrasound and magnetic resonance imaging, have been used with some success to supplement mammography in certain specific cases. For example, ultrasound can be used to determine whether a lesion detected by a mammogram is a liquid cyst or a solid tumor. However, even with the combined use of mammography, ultrasound, and

MRI techniques, the current method of screening for breast cancer does not meet the ideal requirements of the IOM report. Therefore, researchers are actively searching for alternative modalities of screening and diagnostic breast imaging.[7]

1.2.1 The motivation of the project

Traditionally breast cancer is image using x-ray and ultrasound both have Sideffects :

- X-ray is an ionized type of radiation (harmful if repeated many times).
- Ultrasound requires coupling medium or a jell which was be inconvenience to the patient (patient can only carry out imaging in a clinic or hospital).
- Our proposed microstrip patch will have high patch impedance compatible with that of the skin tissue (does not require coupling agent and transmit low power EM signal).

1.2.2 Goals of the project

- To utilize a microstrip patch antenna for medical application.
- The conceptual design is used for imaging breast tissues infected with benign and malignant cancer.
- We propose a patch on an FR4 (1.6mm thick) dielectric substrate is fed with a 50 Ω transmission line placed at a resonant frequency 2.45 GHz.
- We will design, fabricate, and measure the antenna with a synthetic breast tissue placed on top of it.

1.3 Structure of Microstrip Antennas

A microstrip antenna in its simplest configuration consists of a radiating patch on one side of a dielectric substrate which has a ground plane on the other side. The patch conductors, normally of copper or gold, can assume any shape, but regular shapes are generally used to simplify analysis and performance prediction. Various types of substrate materials have a large range of dielectric constant and loss tangent values have been developed.[8]

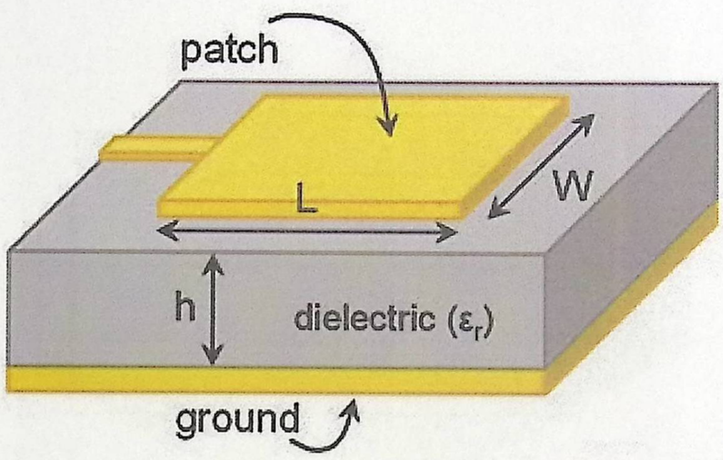

Figure 1.3.1: Cross section of microstrip antenna.

1.4 Technologies

1.4.1 Ansoft HFSS software

HFSS is High Frequency Structure Simulator that provides the full 3D simulation in the field of Electromagnetics. You can validate and analyze the design of any type of Antenna, Microwave Circuit. It also provides the Electromagnetic Compatibility (EMC) Test and Specific Absorption Rate (SAR) Analysis. The newbies are advised to straight away start with the help provided which contains a lot of useful material. The good thing about HFSS is that the results are very accurate. The HFSS design can easily be exported to other Simulators like CST Microwave Studio and can be validated there as well.

With this program we can build the required antenna ,then given the estimated result when we fabricate the antenna by applying our antennas parameters (highest, length , width , dielectric constant) to give us an important information , such as return loss ,gain , bandwidth, radiation pattern , and VSWR , that will we need in our project, when we supply a source power to feed a simulator antenna design .

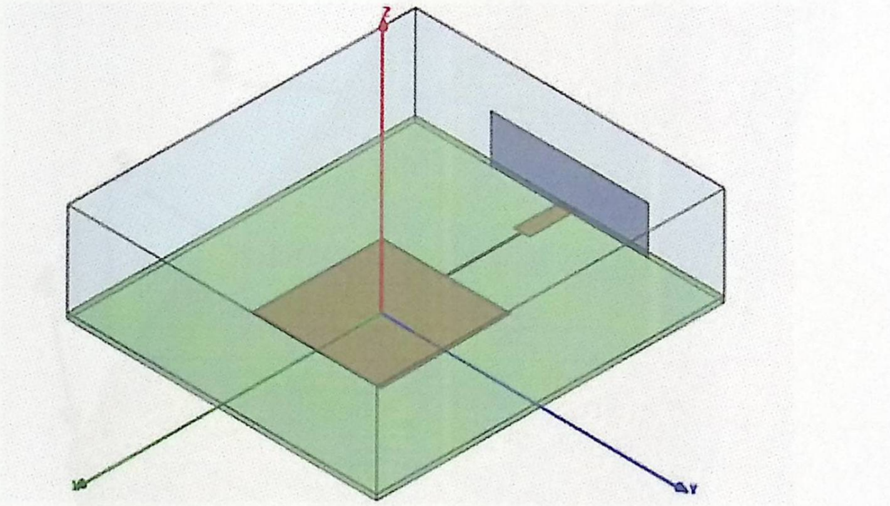

Figure 1.4.1: HFSS microstrip antenna simulation design.

1.5 Breast Cancer: Anatomy, Histology, and Pathology.

In the development of an alternative modality of breast cancer screening, it is important to have a basic understanding of the anatomy, histology, and pathology of the breast.

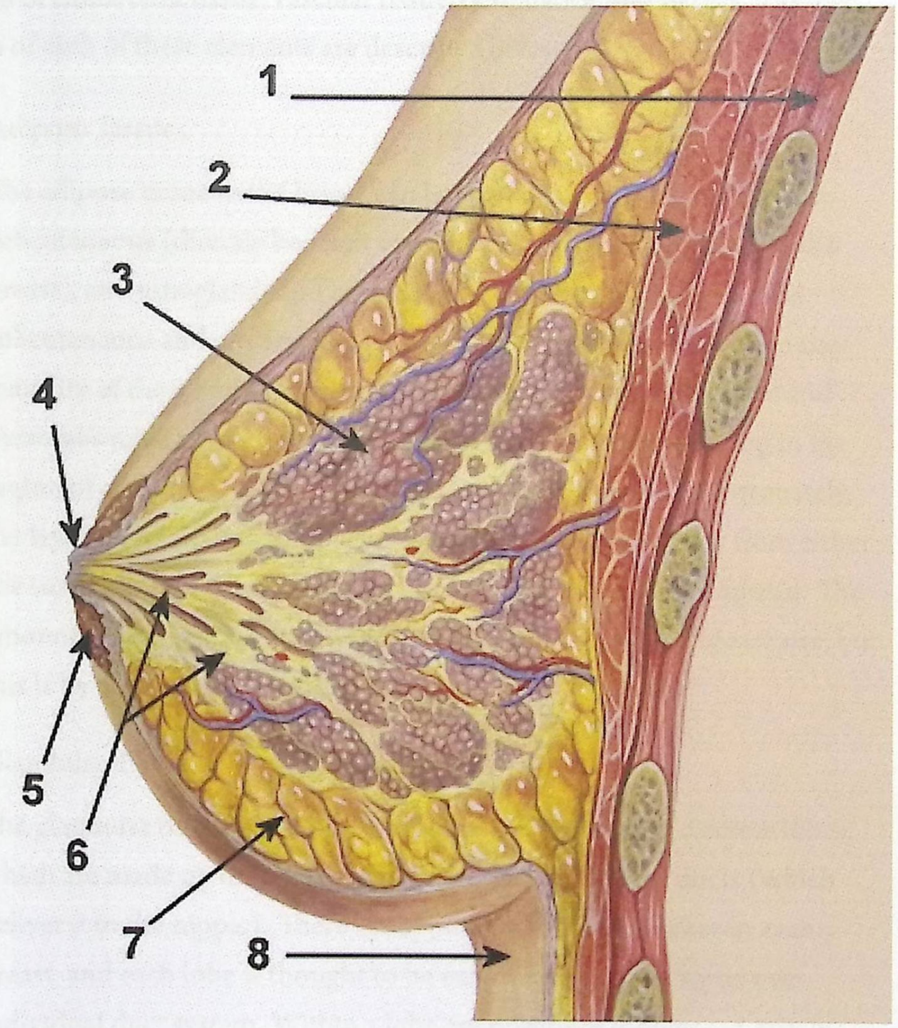

Figure 1.5.1: Anatomy of the Breast: 1. Chest wall 2. Pectoralis muscles 3. Lobules 4. Nipple 5. Areola 6. Ducts 7. Fatty tissue 8. Skin [9] .

1.5.1 Anatomy

The breast (see Figure 1.5.1) is a modified skin gland that lies on the chest wall, usually between the clavicle and the sixth rib, and is bounded externally by skin and internally by the pectoralis muscle. Breast tissue also extends up into the axilla (underarm region) via a pyramidal-shaped axillary tail. The tissue in the breast primarily consists of a combination of fat and glandular tissue, with the relative proportions of the two varying widely. The remainder of the breast is made up of connective tissue, vascular tissue, lymphatics, and nerves. The key features of each of these elements are described below.

1. Adipose Tissue .

   The adipose tissue in the breast can be divided into three main groups: subcutaneous (directly beneath the skin), retromammary (back of the breast), and intraglandular (between the glandular structures). The subcutaneous and retromammary fat regions form a layer between the majority of the glandular tissue and the external boundaries (skin and pectoralis muscle) of the breast. The majority of cancers develop in the region of glandular tissue within 1 cm of these fat layers. Unfortunately, the layers of fat do not completely isolate the glandular tissue from either the surrounding skin or muscle, which enables the cancer to spread. The amount of fat generally increases with age, body mass, and breast size, but this is by no means an absolute .[10]

2. Glandular Tissue .

   The glandular tissue in the breast consists of a number of discrete lobes, which are made up of lobules (which produce milk) and ducts (which deliver it to the nipple). There are approximately 15-20 lobes in each breast, and each lobe is thought to be exclusively drained by its own individual duct system. Within a lobe are dozens of lobules 2-3 mm in diameter, and within each lobule are as many as 100 alveoli (often referred to as acini), which are the basic secretory units of the breast. The ductal system can be thought of as a tree-like structure, with a single lactiferous duct that opens at the nipple acting as a trunk that branches into many smaller ducts that each end in what has been termed the terminal duct lobular unit (TDLU) .[11]

3. Other Tissue .

Skin and Connective Tissue.

The breast is supported by a combination of connective tissue and skin. The skin overlying the breast generally varies in thickness between 0.8mm and 3mm, and skin thickness tends to be inversely proportional to breast size. The skin also contains the nipple, which is slightly below the centerpoint of the breast and extends about 5-10mm above the skin surface, and the surrounding areola, which contains a number of small bumps called Montgomery's glands, which lubricate the skin during breast feeding. Finally, the breast is supported by a surrounding layer of fascia (connective tissue), which is interspersed with the subcutaneous and retromammary adipose tissue, and by a number of suspensory ligaments (Cooper's ligaments) that provide an internal supporting framework for the breast lobes . [11]

Vascular and Nerve Tissue.

The breast receives its blood supply from a variety of axillary, internal thoracic, and intercostal arteries. Each artery generally has a corresponding veinous channel which drains a web of veins originating from the nipple, the subcutaneous layer, and the glandular tissue of the breast. Similarly, the breast receives its nerve supply from multiple branches of the intercostal nerves .[12]

Lymphatic Tissue.

The lymphatics, vein-like vessels that drain lymph fluid into the blood stream, represent the body's main line of defense in the body's immune response, but they also provide a conduit for cancer cells to spread and metastasize. In the breast, the vast majority of lymphatics travel from the nipple to lymph nodes in the axilla, and from there to nodes above the collar bone. Some lymphatics also drain the rear part of the breast to nodes under the breast bone (internal thoracic nodes). Finally, there are also a small number of lymph nodes within the breast itself.[13]

1.5.2 Histology and Pathology.

Under normal, healthy, conditions, both the ductal and lobular cells in the breast are lined with a specialized two-layer cell lining that is attached to a basement membrane. The inner layer is made up of epithelial cells that perform secretory and absorptive functions, while the outer layer is made up of contractile myoepithelial cells [16]. It is in this cell lining where cancer is thought to originate, and the status of these cells is often critical in distinguishing benign diseases from malignancy.

1. Benign Disorders of the Breast.

   Approximately 90 percent of lumps and suspicious breast lesions turn out to be one of a variety of benign breast disorders. These disorders include breast cysts, adenomas, fibroadenomas, papillomas, fat necrosis, mammary duct ectasia, and epithelial hyperplasia. A brief description of some of the more common benign conditions follows.

   Cysts, Fibroadenomas, and Adenomas.

   Cysts are found throughout the body and are generally fluid-filled sacs that are lined with cells that actively produce secretions that fill the cyst. Breast cysts are different in that they are in fact closed-off portions of mammary ducts that passively fill with fluid. Breast cysts are round, smoothly contoured, and are generally movable. Often, they are detected by mammogram or palpation, but are later diagnosed by ultrasound or biopsy. Like cysts, fibroadenomas present as round, smoothly contoured, movable lumps. These benign tumors are made of epithelial and stromal cells, which gives them a firm, but not hard, consistency. They are generally solitary (in 80 percent of cases), and rarely exceed 3cm in diameter. Fibroadenomas have been shown to have malignant changes in about 0.1

percent of cases (mostly in the form of LCIS) . True adenomas (or tubular adenomas) are neoplastic tumors that are composed of tubular structures lined by a single layer of epithelial cells. They tend to form sharply circumscribed nodules roughly 2 cm in size. Adenomas occur much less frequently than fibroadenomas, but are more likely to be mistaken for cancer in screening. Biopsy showing the presence of actin is used to distinguish this benign tumor from cancer .

Papillomas and Mammary Duct Ectasia.

Papillomas and mammary duct ectasia are disorders of the ducts that often lead to nipple discharge. Intraductal papillomas are small polyp-like growths in the ducts directly behind the nipple which often cause a watery, bloody discharge from the nipple. Mammary duct ectasia is a disorder that causes the ducts to become distended and clogged, often causing a lump, swelling, and nipple discharge. While these conditions cause discharge, one of the signs of malignancy, both papillomas and mammary duct ectasia are benign conditions.

Fat Necrosis.

Fat necrosis is a condition, commonly associated with trauma, that occurs when a group of cells in the breast dies, leaving behind a small, hard, flat lesion. Although necrosis is often a sign of malignancy, this condition is distinguished from carcinoma by its yellow color and the bulge it typically forms in the adipose tissue .

Epithelial Hyperplasia.

Epithelial hyperplasia is the generic term for the proliferation of the epithelial cells that line the ducts and lobules in the breast. Epithelial hyperplasia can be classified by its severity: mild (three to four cells thick), moderate (more than four cells), florid (completely filling the lumen), and atypical (any proliferation that shows signs of potential malignancy). Hyperplasia in the breast is distinguished from neoplasia (the process underlying malignancy) by the following features: uniformity of the nuclei, the presence of myoepithelial cells, and absence of necrosis. When additional conditions are present alongside epithelial hyperplasia (such as papilloma, mammary duct ectasia, or fat necrosis), it can become diagnostically difficult to distinguish from carcinoma, but the presence of myoepithelial cells and uniform nuclei would still suggest benignancy . Although epithelial hyperplasia is a benign condition, studies have shown an association with an increased risk for the development of carcinoma. Patients with moderate and florid hyperplasia have a slightly increased risk (1.5-2 times), and those with atypical hyperplasia are five times more likely to develop carcinoma .

2. Cancers of the Breast .

Breast cancer comes in many forms, and is distinguished by the type of tissue where the malignancy originates and whether the cancer is confined to that original site. If the cancer originates in the lobules that manufacture milk or the ducts that carry it, as most commonly occurs, it is classified as carcinoma of the breast. Cancers that originate in the muscle, fat, or connective tissue in the breast are referred to as sarcomas. If the cancer is confined to its original site, and has not yet formed a tumor mass, it is referred to as in situ cancer, otherwise, it is considered to be infiltrating. Furthermore, if the cancer has spread beyond the breast and its associated lymph nodes to distant parts of the body, it is said to have metastasized. There is considerable debate over whether breast cancer develops in a continuous progression from epithelial hyperplasia to carcinoma in situ and finally to infiltrating carcinoma (see Figure 1.5.2), or if each condition develops independently. Although there is considerable evidence to support the theory of progression, to date there has been no scientific proof. In any case, studies have shown conclusively that those with atypical hyperplasia and DCIS are at increased risk for invasive carcinoma.

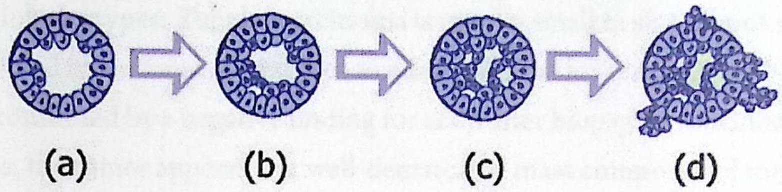

Figure 1.5.2: (a) Mild Epithelial Hyperplasia (b) Atypical Epithelial Hyperplasia (c) Carcinoma In Situ (d) Infiltrating Carcinoma (Adapted from) .

Ductal Carcinoma in situ.

Ductal Carcinoma in situ (DCIS) comes in many forms, which are classified based upon the patterns the cancer cells form. As the 24 cancer cells lining the ductal wall proliferate, they begin to fill the inner space of the duct: first with small protrusions (micropapillary DCIS), then larger ones (papillary DCIS); sometimes the protrusions form a lattice structure (cribriform DCIS) and in others the duct is entirely filled (solid DCIS). In the most severe cases, the center cells die, forming a necrotic core (comedo DCIS) .

Lobular Carcinoma in situ.

In Lobular Carcinoma in situ (LCIS), the lobules are completely filled by round, uniform, medium-sized cells. Occurrences of atypia, pleomorphism, and necrosis are also found infrequently in LCIS. Since LCIS cannot be detected by palpation and is unlikely to appear on a mammogram, it is usually discovered as an incidental finding in breast tissue that has already been removed due to suspicion of other disease. Statistically, LCIS is bilateral in about 30 percent of cases and the majority of cases are found within 5 cm of the skin surface near the nipple .

Infiltrating Carcinomas.

Of the carcinomas of the breast, the vast majority (85 percent) form in the ducts, while the remaining fifteen percent form in the lobules. Since the majority of ductal and lobular cells are found in the upper part of the breast, the center of the breast, or in the outer quadrant, this is also where most cancers occur. Other, less common, invasive carcinomas include tubular carcinoma, mucinous carcinoma, and medullary carcinoma, all of which have better prognoses than the ductal or lobular types. Tubular carcinoma is usually small in size (about 1 cm in diameter) and is similar in appearance to adenomas but lacks myoepithelial cells, which is confirmed by a negative finding for actin after biopsy. In mucinous carcinoma, the tumor appears as a well-demarcated mass composed of tumor cells floating in pools of mucin. Medullary carcinoma is characterized by a solid mass with a well-defined border that contains diffuse clusters of large, pleomorphic tumor cells that have been infiltrated by lymphocytes. Finally, invasive carcinomas may be termed inflammatory, which describes the condition that occurs when the cancer has extensively spread to the dermal lymphatics, causing edema, tenderness, and swelling of the breast. The prognosis of inflammatory carcinomas is generally quite poor .

Infiltrating Ductal Carcinoma.

Infiltrating ductal carcinoma is the most common type of breast cancer, accounting for about 75 percent of all breast cancer, and is the most common lethal cancer of the breast. In this invasive form of breast cancer, the malignant cells break through the basement membrane of the mammary duct into the surrounding fatty tissue. This leads to the growth of fibrous, scarlike tissue around the cancer cells, which can be detected both on a mammogram and by palpation .

Infiltrating Lobular Carcinoma.

Unlike the ductal form, this invading carcinoma does not provoke the growth of fibrous tissue and tends to infiltrate in a more diffuse manner, forming single file groupings of malignancy in the surrounding tissue. As a result, it is much more difficult to detect on a mammogram and often feels more like a thickening of tissue rather than a lump. Unfortunately, this means that it is usually detected at a later stage than its ductal counterpart.

Sarcomas and Other Rare Types.

There are a variety of sarcomas (all rare) that may occur in the breast, including angiosarcoma (sarcoma of blood or lymphatic vessels), fibrosarcoma (sarcoma of connective tissue), liposarcoma (sarcoma of adipose tissue), osteosarcoma (bone forming sarcoma), and chondrosarcoma (cartilage forming sarcoma). One of the more common sarcomas found in the breast is Phyllodes tumor (formerly called cytosarcoma Phyllodes), which mostly tends to affect younger women. Phyllodes tumors can grow as large as 15cm and are similar in appearance to fibroadenomas. These tumors often recur locally, but rarely metastasize. Finally, breast tumors can also form as a result of other cancers such as lymphoma and leukemia, or due to metastases from cancers such as melanoma and lung cancer; however, all of these are very rare .[12]

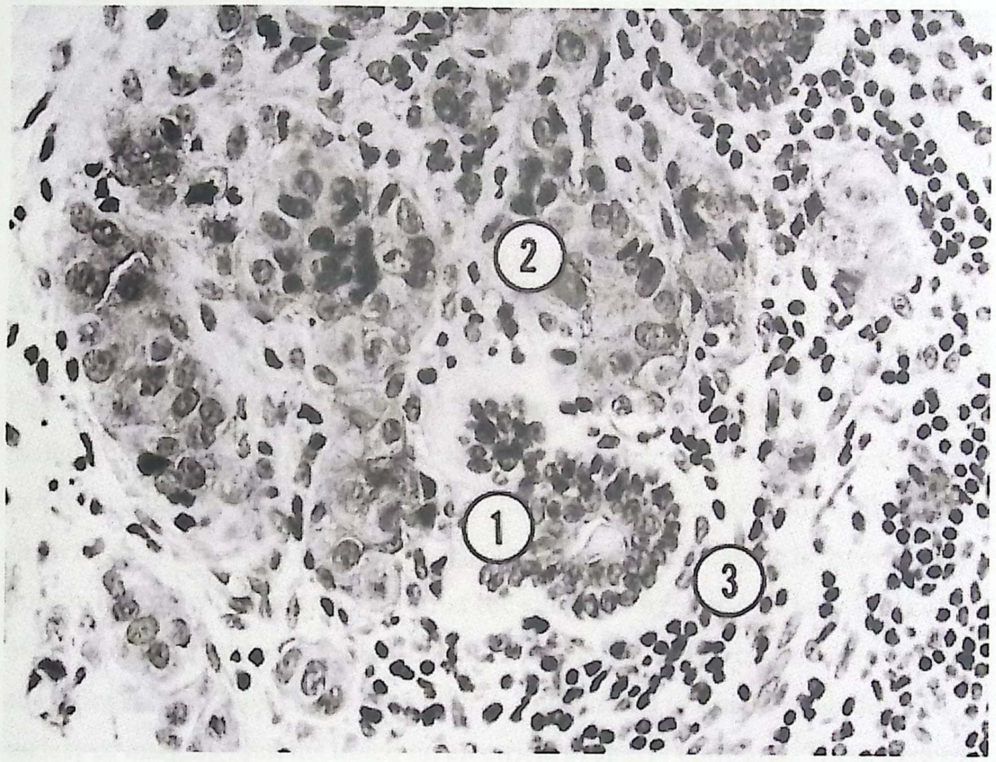

Figure 1.5.3: Infiltrating Ductal Carcinoma. (1) Cancer cells surrounding a normal duct. Cancer cells (2) are larger and more irregular than normal cells (3).

1.6 General Theory of Microwave Imaging.

The fundamental basis of any breast imaging system is the contrast that exists between the material properties of healthy and malignant tissue. As mentioned previously, the current methods commonly used in clinical applications rely on contrast in density (x-ray), acoustic impedance (ultrasound), and nuclear spin relaxation (MRI). However, an additional source of measurable contrast arises from the different electrical properties of healthy and malignant breast tissue.

1.6.1 Electrical Properties of Human Breast Tissue .

The theoretical basis for microwave breast imaging is the high contrast between the permittivity and conductivity of healthy and malignant breast tissue. This contrast has been documented in a variety of studies [14, 15, 16, 17, 18, 19]. Figure 1.6.1 shows graphs of conductivity and relative permittivity of normal and malignant breast tissue over the microwave frequency range. While there is variation among the values reported by the different research groups, all studies show substantial contrast. This suggests that microwave imaging is theoretically possible at many frequencies, and that the choice of frequency is largely a matter of balancing the added spatial resolution afforded by higher frequencies with the additional attenuation that comes with it. This has led to the investigation of a variety of imaging systems based on electrical property contrasts. These systems include the aforementioned microwave-induced thermoacoustic imaging, EIT, and MWI systems.

1.6.2 Active Microwave Imaging .

In general, active microwave imaging falls under the broad category of inverse problem. The objective of MWI is to reconstruct the unknown distribution of the complex permittivity inside the mammary tissue given a set of data measured

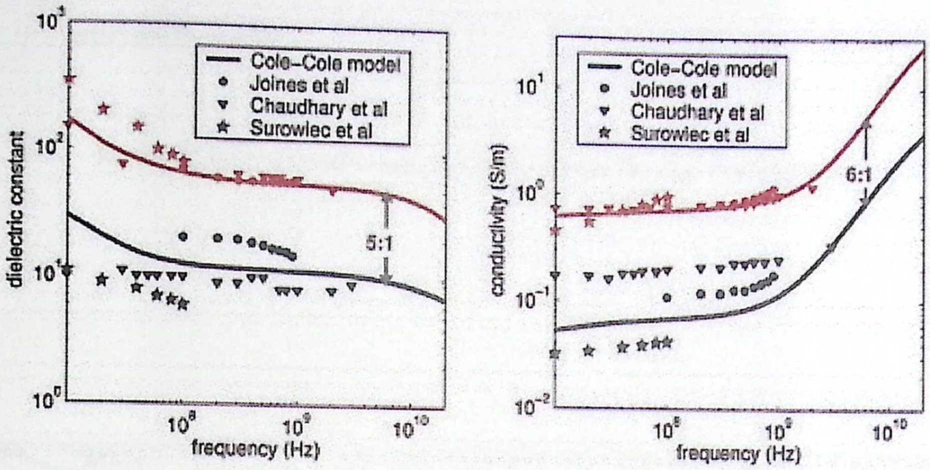

Figure 1.6.1: Measured Contrast from Several Studies. Black: Normal, Red: Malignant .[20]

along the perimeter of the volume. There are several groups currently performing research in active microwave imaging [21].

While these systems take varying approaches to the specifics of data acquisition and image reconstruction, they share the common potential advantages that microwave imaging offers over traditional mammography. First, active microwave imaging systems do not require the use of ionizing radiation. In addition, MWI systems would eliminate the need for uncomfortable breast compression. Furthermore, microwave imaging systems should be less expensive than x-ray systems and much less costly than MRI. All of these characteristics would allow for earlier and more frequent examinations. Finally, microwave imaging has the potential for a much higher sensitivity in detecting tumors, as well as higher specificity in differentiating malignant and benign tumors. This is due to the fact that the electrical contrast is likely to be much higher than the density contrast, particularly for malignant lesions.

1.7 PROJECT PLAN

Table 1.7.1: overall system timing table for the first semester

Week / Task	1	2	3	4	5	6	7	8	9	10	11	12	13	14	15
Select the idea	■	■													
Preparing for the project and collecting information			■	■	■	■	■	■	■	■	■	■	■		
Project analysis				■	■	■									
Determine the project equipment & requirements						■	■	■	■	■					
Design and analysis				■	■	■	■	■	■	■	■	■			
Dr. Osama's Deadline													■		
Submit the report to electrical engineering department														■	

Do all the good you can. By all the means you can. In all the ways you can. In all the places you can. At all the times you can. To all the people you can. As long as ever you can.

John Wesley

2

Microstrip Antennas

2.1 Definition of Microstrip Antennas

A microstrip antenna in its simplest configuration consists of a radiating patch on one side of a dielectric substrate (ε_r<10) , which has a ground plane on the other side. The patch conductors normally of copper and gold, can assume virtually any shape, but conventional shapes are generally used to simplify analysis and performance prediction . The dielectric constant (ε_r) of the substrate should be low (ε_r=2.5) to enhance the fringe fields which account for the radiation . However, various types of substrates having a large range of dielectric constant and loss tangents have been developed.

2.1.1 Advantages of Microstrip Antennas

1. Light weight, low volume.

2. Low fabrication cost.

3. The antenna may be easily mounted on missiles, rockets and satellites without major alterations.

4. The antennas have low scattering cross section.

5. Linear or circular polarization is possible with simple changes in feed position.

6. Dual frequency antennas easily made.

7. No cavity backing required.

8. Microstrip antennas are compatible with modular designs (solid state devices such as oscillators, amplifiers, variable attenuators, switches, modulators, mixers, phase shifters etc. can be added directly to antenna substrate board).

9. Feed lines and matching networks are fabricated simultaneously with the antenna structure.

10. Mechanically robust.

2.1.2 Disadvantages of Microstrip Antennas

1. Narrow bandwidth.

2. Most microstrip antennas radiate into a half plane.

3. Practical limitations on the maximum gain (20dB).

4. Poor end fire radiation performance.

5. Poor isolation between the feed and the radiating elements.

6. Low efficiency.

7. Poor polarization purity.

8. High Q (sometime in excess of 100).

2.1.3 Applications of Microstrip Antennas

1. Radars.

2. Radio altimeter.

3. Missile telemetry.

4. Weapon fusing.

5. Feed elements in complex antennas.

6. Biomedical radiator.

7. Mobile communication.

2.2 Various Microstrip Antenna Configurations

Microstrip antennas are characterized by more physical parameters than are conventional microwave antennas. They may be of any geometrical shape and any dimension. However, all microstrip antennas can be divided into three basic categories: microstrip patch antennas, microstrip traveling-wave antennas and microstrip slot antennas. Their characteristics are considered below.

2.2.1 Microstrip Patch Antennas

A microstrip Patch Antenna (MPA) consists of a conducting patch of any planar geometry on one side of a dielectric substrate backed by a ground plane on the other side. There are virtually an unlimited number of patches patterns for which radiation characteristics may be calculated. figure 2.2.1, and figure 2.2.2 show some microstrip patch antenna configuration.

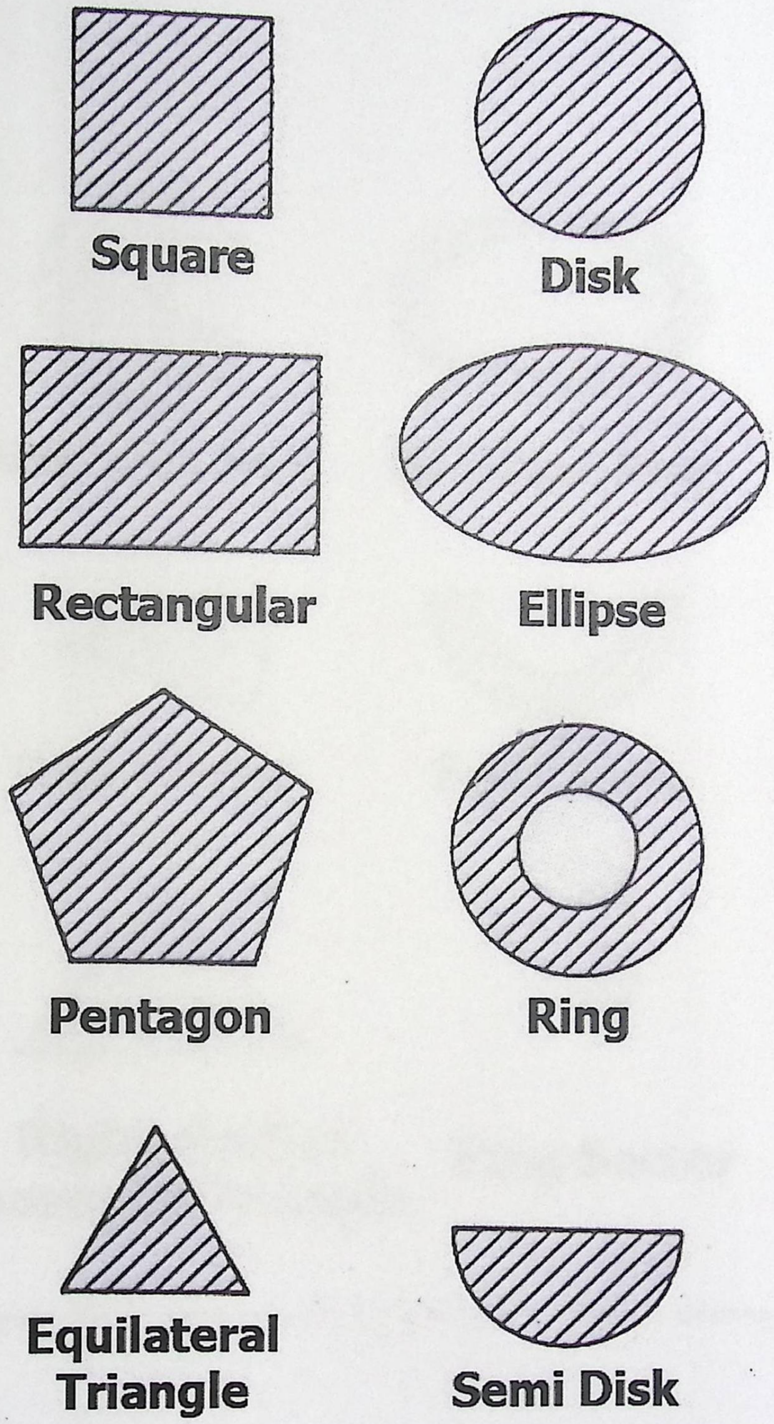

Figure 2.2.1: Various microstrip patch antenna configurations

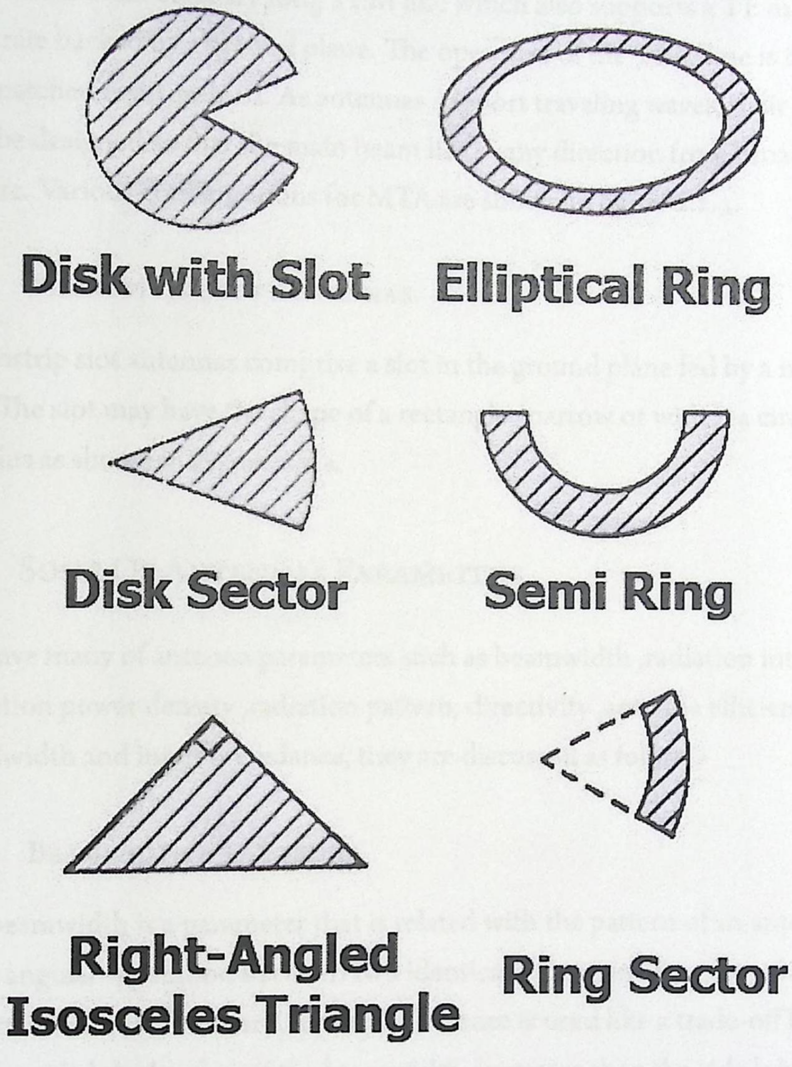

Figure 2.2.2: Other possible geometries for microstrip antennas.

2.2.2 Microstrip Traveling-Wave Antennas

Microstrip traveling-wave antennas (MTA) consist of chain-shaped periodic conductors or an ordinary long TEM line which also supports a TE mode, on a substrate backed by a ground plane. The open end of the TEM line is terminated in a matched resistive load. As antennas support traveling waves, their structures may be designed so that the main beam lies in any direction from broadside to endfire. Various configurations for MTA are shown in figure 2.2.3.

2.2.3 Microstrip Slot Antennas

Microstrip slot antennas comprise a slot in the ground plane fed by a microstrip line. The slot may have the shape of a rectangle (narrow or wide), a circle or an annulus as shown in Figure 2.2.4.

2.3 Some Of Antenna's Parameters

We have many of antenna parameters such as beamwidth ,radiation intensity ,radiation power density ,radiation pattern, directivity ,antenna efficiency ,gain ,bandwidth and input impedance, they are discussed as follow:-

2.3.1 Beamwidth of antenna

The beamwidth is a parameter that is related with the pattern of an antenna, and is the angular separation between two identical points on opposite sides of the pattern maximum. It is very important because is used like a trade-off between it and the side lobe level, so if the beamwidth decreases then the side lobe increases and vice versa. One of the most used beamwidth is the "half-power beamwidth" (HPBW), and is the angle at which the main lobe has half of its power. We have also the "first-null beamwidth" (FNBW) and it is the angular separation between the first nulls of the pattern.

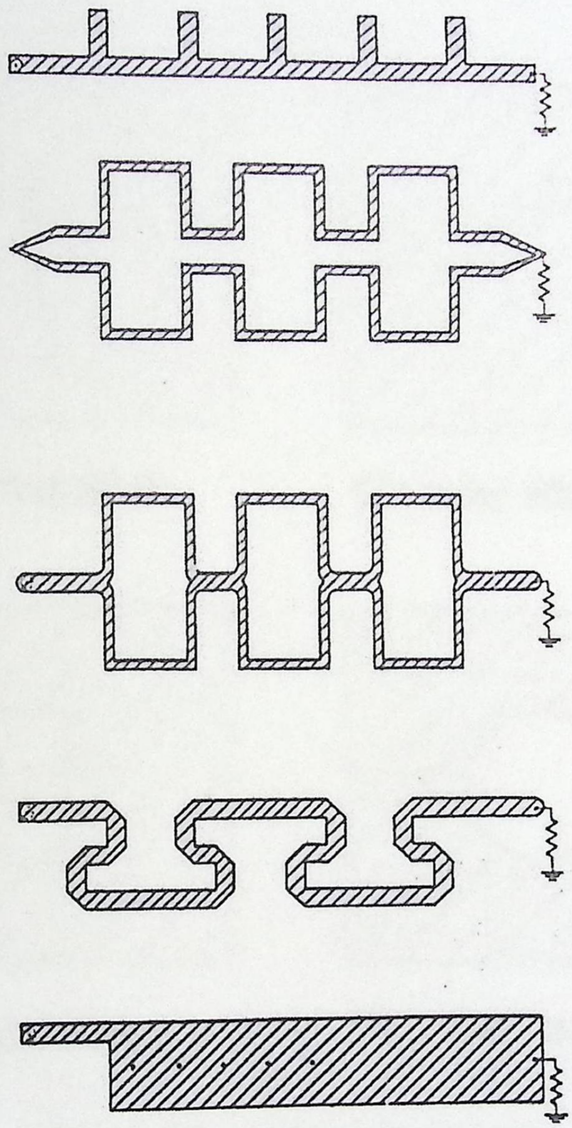

Figure 2.2.3: Microstrip traveling wave antennas.

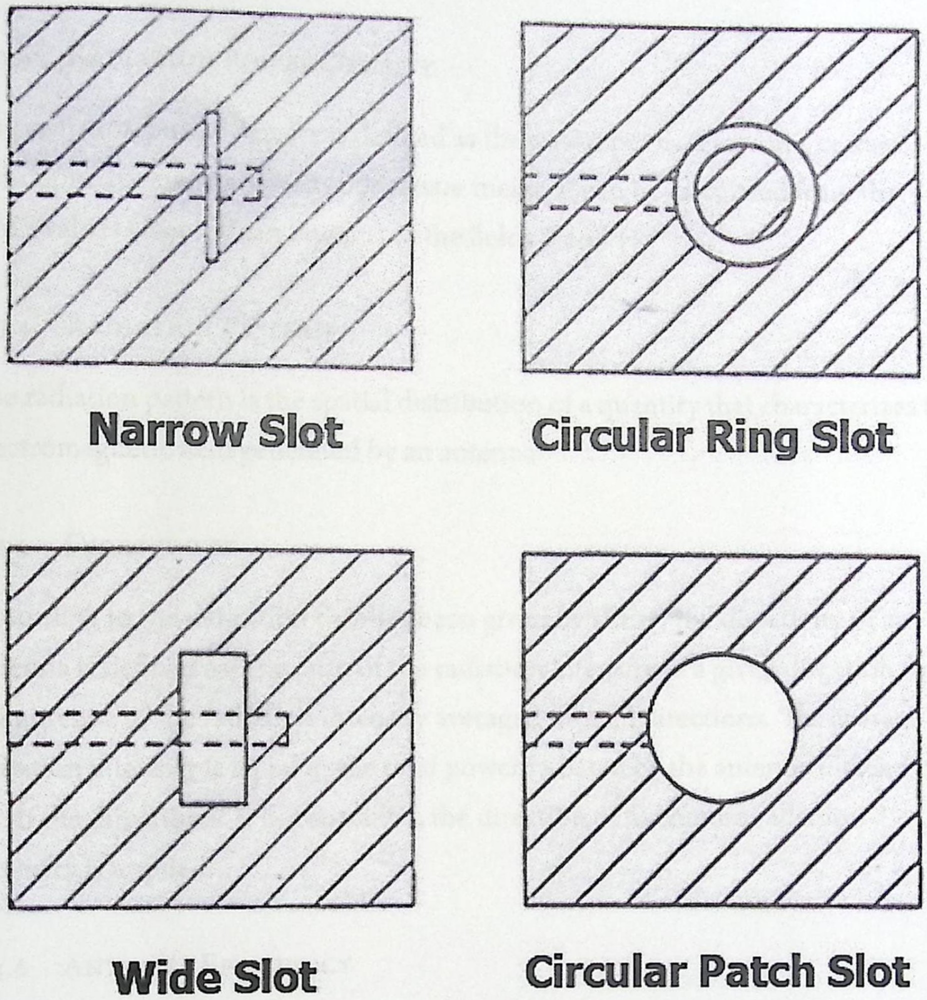

Figure 2.2.4: Microstrip slot antennas.

2.3.2 Radiation Intensity

It is defined as the power radiated from an antenna per unit solid angle. Its units are watts per steradian. This parameter, in large distances, has the property of being independent of the distance that the antenna is.

2.3.3 Radiation Power Density

The radiation power density is defined as the power per unit area in a certain direction. The units are watts per square meter. It can be calculated from the RMS values (Root Mean Square) of the fields E and H.

2.3.4 Radiation Pattern

The radiation pattern is the spatial distribution of a quantity that characterizes the electromagnetic field generated by an antenna.

2.3.5 Directivity

According to the definition that has been given by IEEE , the directivity of an antenna is defined as "the ratio of the radiation intensity in a given direction from the antenna to the radiation intensity averaged over all directions. The average radiation intensity is equal to the total power radiated by the antenna divided by 4π. If the direction it is not specified, the direction of maximum radiation intensity is implied.

2.3.6 Antenna Efficiency

The total antenna efficiency takes into account the ohmic losses of the antenna through the dielectric material, the reflective losses at the input terminals and losses within the structure of the antenna.

2.3.7 Gain

Gain is a useful measure that helps to describe the performance of an antenna. It is defined by IEEE as "the ratio of the intensity, in a given direction, to the radiation intensity that would be obtained if the power accepted by the antenna were radiated isotropically .The gain it is linearly related with the directivity measurement through the antenna radiation efficiency.

2.3.8 Bandwidth

We cannot build an infinite antenna, so due to it finite geometry, the antenna is limited to operate successfully in a band or frequency range and this frequency range is known as bandwidth. For narrowband antennas, the bandwidth can be specified as the ratio of the frequency range in which the specifications are met and the center frequency.[22]

2.3.9 Input Impedance

The input impedance of the antenna (ZA) is the relationship between voltage and current at the input terminals of the antenna, with no load attached. The input impedance of an antenna is generally a function of frequency, so the relationship between voltage-current at the input of the antenna depends on the frequency, and ZA depend also on the frequency. If at a given frequency, the reactance of the input impedance antenna is equal to zero, it is said that the antenna is resonant at that frequency.

2.4 Feeding Methods of Single Element

There are many configurations that can be used to feed microstrip antennas. The four most popular are: the microstrip line feed, coaxial probe feed, aperture coupling feed and proximity coupling feed. Microstrip line feed is easy to fabricate, simple to match by controlling the inset position and relatively simple to model. However, as the substrate thickness increases surface waves and

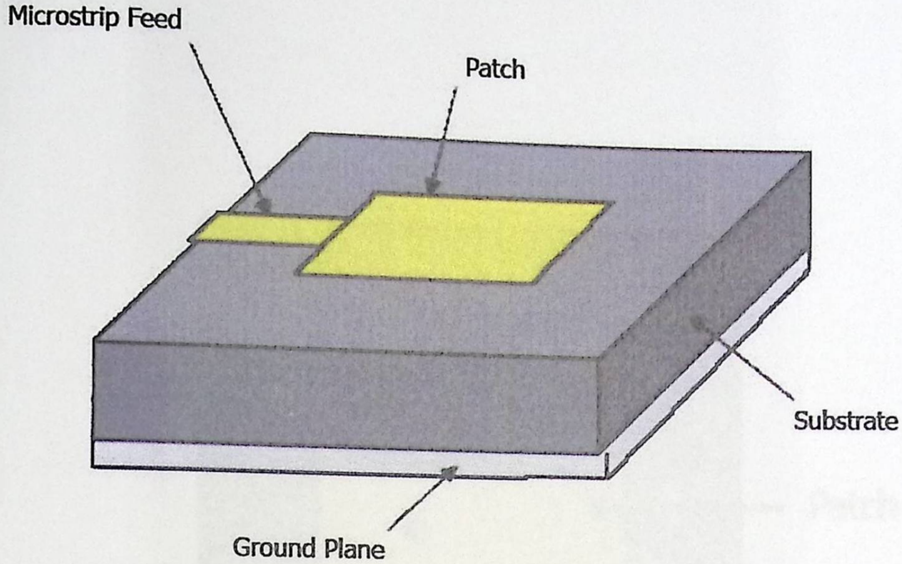

Figure 2.4.1: Microstrip feed.

spurious feed radiation increase. Coaxial probe feed is also easy to fabricate, low spurious radiation, but difficult to model accurately and has a narrow bandwidth of impedance matching.[23]

Aperture coupling constant of two substrates separated by a ground plane. On the bottom side of the lower substrate there is a microstrip feed line whose energy is coupled to the patch through a slot on the ground plane. It is easier to model and has little spurious radiation. The proximity coupling has the largest band width, is some what easy to model and has low spurious radiation.

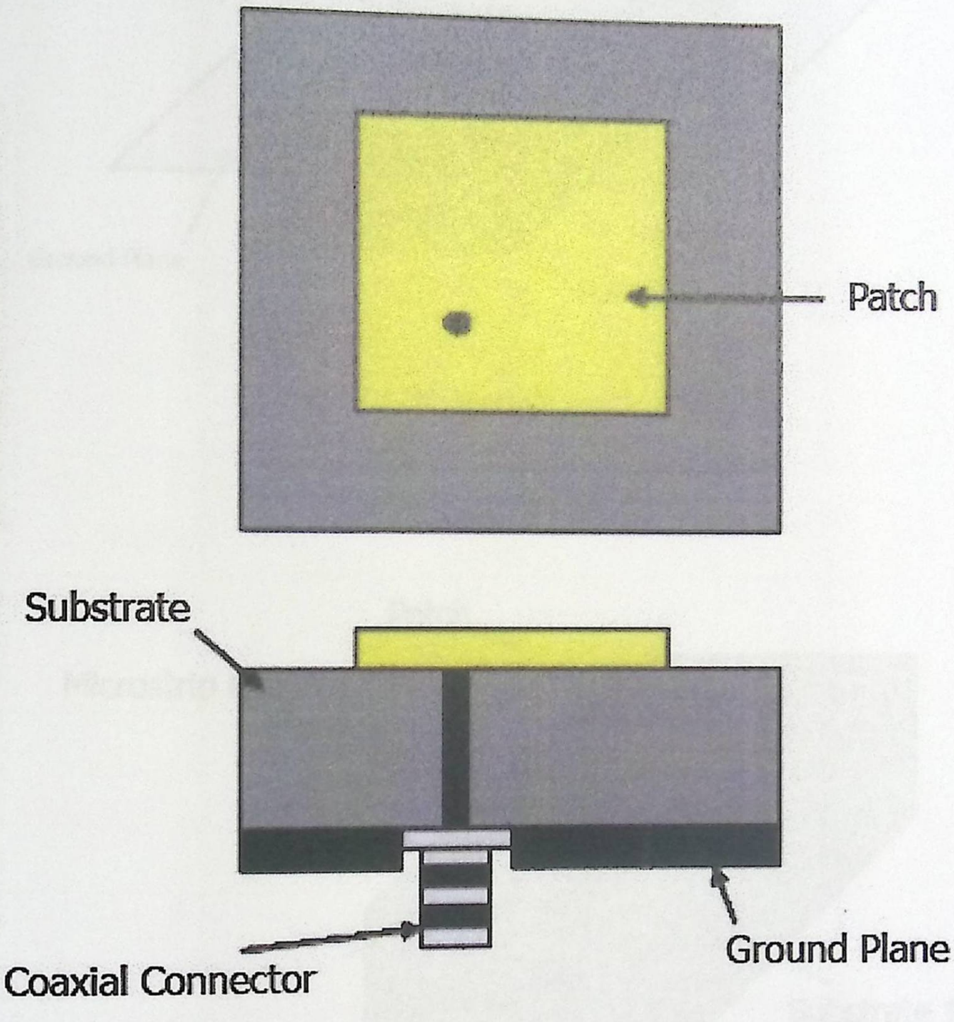

Figure 2.4.2: Coaxial probe feed.

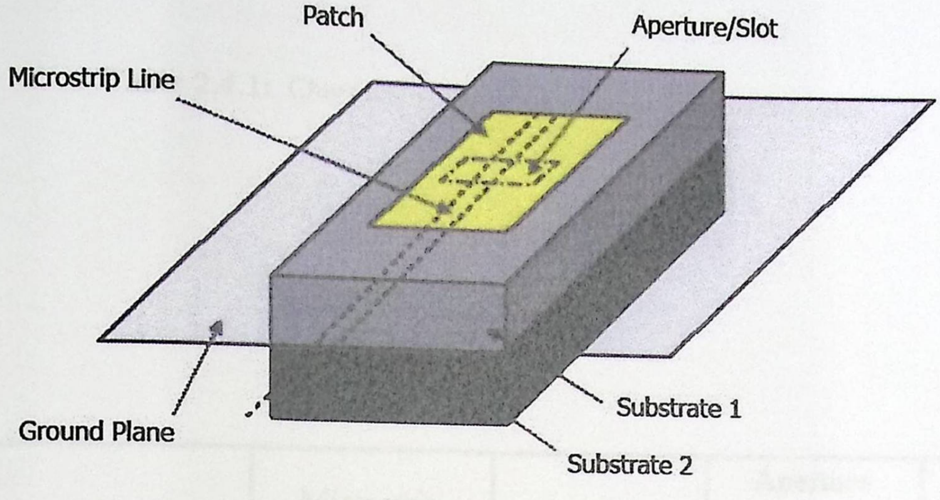

Figure 2.4.3: Aperture coupling feed.

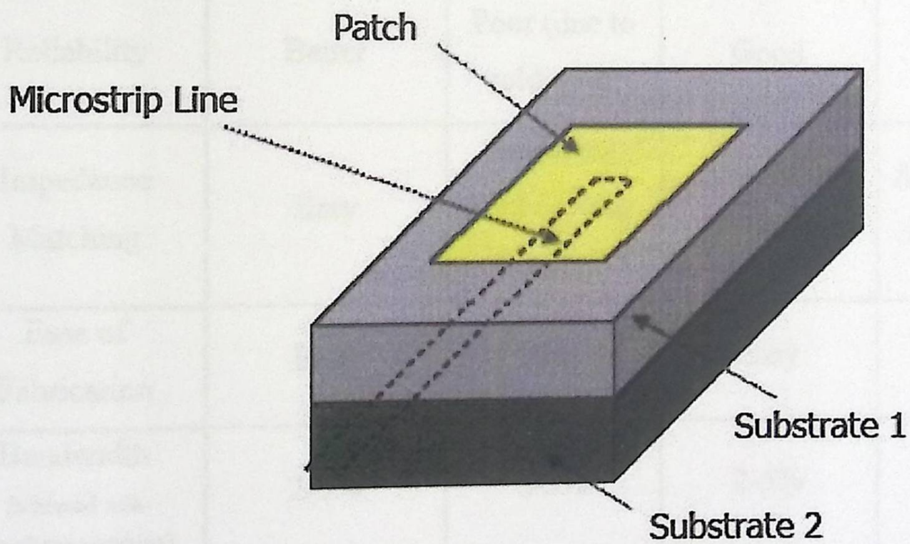

Figure 2.4.4: Proximity coupling feed.

Table 2.4.1: Characteristics of the different feed techniques

Characteristics	Microstrip Line Feed	Coaxial Feed	Aperture Coupled Feed	Proximity Coupled Feed
Spurious Feed Radiation	More	More	Less	Minimum
Reliability	Better	Poor (due to soldering)	Good	Good
Impedance Matching	Easy	Soldering and drilling needed	Alignment required	Alignment required
Ease of Fabrication	Easy	Easy	Easy	Easy
Bandwidth (achieved with impedance matching)	2-5%	2-5%	2-5%	13%

Do you want to be a hero ? Don't be the kind of person who watches others do great things or doesn't know what's happening. Go out and make things happen. The people who get things done have a burning desire to make things happen, get ahead, serve more people, become the best they can possibly be, and help improve the world around them.

Glenn Ekeren

3

Microstrip Theory

3.1 Design methodology

The project consists of two parts. In the first part designing a rectangular patch transmitter microstrip antenna at 2.45 GHz with 50 Ω input impedance to radiate into breast tissues mimic malignant tissues which have high dielectric constant (ε_r=60) compare to the normal tissues to measure the return loss , gain and radiation pattern and the antenna will optimize to achieve lower return loss, higher gain, and better radiation pattern by varying the antenna sizes, adding a matching stub at the input port, and moving the feed port towards the edge to increase the impedance of the antenna. in the second part designing a receiving microstrip antenna identical to transmitter to receive the electromagnetic wave which transmitted through breast tissues and obtain the antenna parameters from it which consist S parameter, radiation pattern , impedance and gain then compare between these parameters in the case of normal and malignant breast tissues.

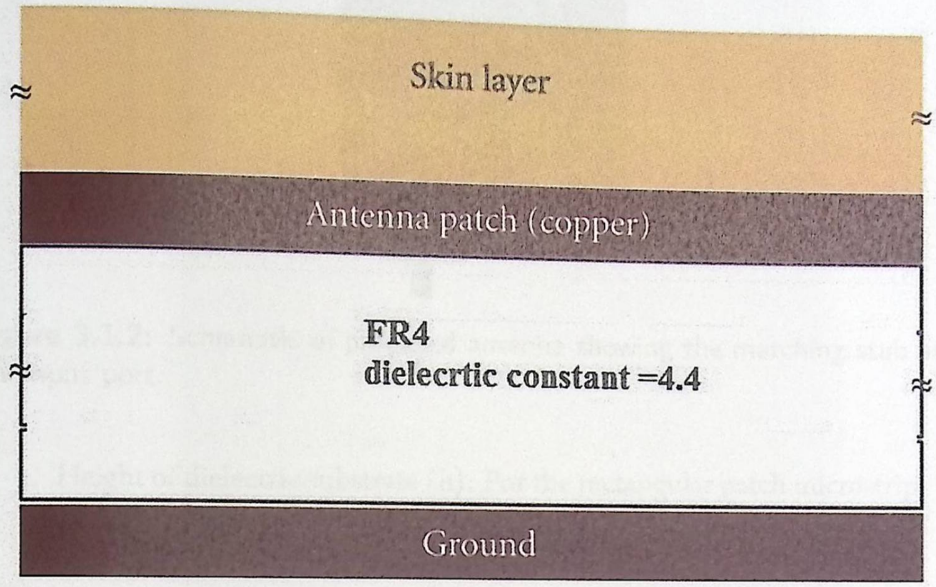

Figure 3.1.1: Schematic of antenna-skin stack.

3.2 Design Specifications

The three essential parameters for the design of a rectangular microstrip Patch Antenna are:

1. Frequency of operation (fo): The resonant frequency of the antenna must be selected appropriately .The resonant frequency selected for this design is 2.45 GHz.
2. Dielectric constant of the substrate (ε_r): The dielectric material is FR4 which has a dielectric constant of 4.4. A substrate with a high dielectric constant has been selected since it reduces the dimensions of the antenna.

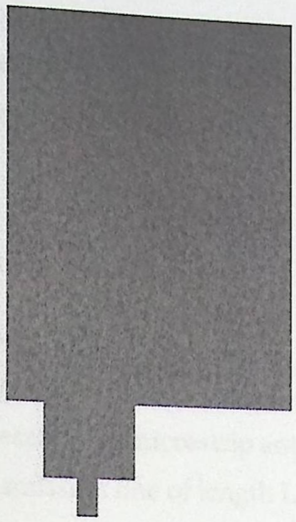

Figure 3.1.2: Schematic of proposed antenna showing the matching stub at the input port.

3. Height of dielectric substrate (h): For the rectangular patch microstrip antenna, the height of the dielectric substrate is selected as 1.6 mm.

Hence, the essential parameters for the design are:

1. fo = 2.45 GHz
2. εr = 4.4
3. h = 1.6 mm

3.3 Methods of Analysis

The most popular models for the analysis of microstrip patch antennas are the transmission line models, cavity model and full wave model (which include primarily integral equations and moment method). The transmission line model is the simplest of all and it gives good physical insight but it is less accurate. The cavity model is more accurate and gives good physical insight but is complex in nature. The full wave models are very accurate very versatile, and can treat single elements with different shapes arrays and coupling. The rectangular patch is the most widely used shapes. It is very easy to analyze using both transmission line and cavity models.[23]

3.3.1 Transmission Line Model

This model represents the microstrip antenna by two slots of width (w) and height (h), separated by a transmission line of length (L). Basically the transmission line model represents the microstrip antenna by two slots separated by a low-impedance (Z) transmission line of length L .[23]

Fringing Effect

Because the dimensions of the patch are finite along the length and width, fields at the edges of the patch undergo fringing. This is illustrated in Figures 3.3.1 (a) and (b), for the two radiation slots of the microstrip antenna. The amount of fringing is a function of the dimensions of the patch and the height of the substrate. Since for microstrip antennas $L/h \gg 1$, fringing is reduced. However, it must be taken into account because it influences the resonant frequency of the antenna. The microstrip is essentially a nonhomogeneous line of two dielectric typically the substrate and air.[23]

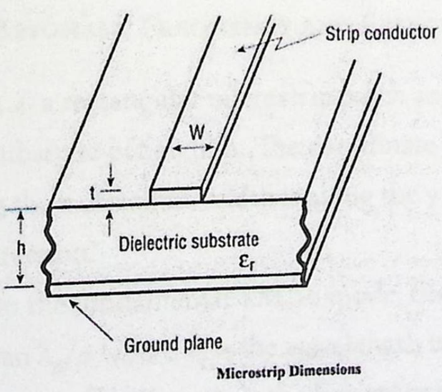

Figure 3.3.1: a. Microstrip Line.

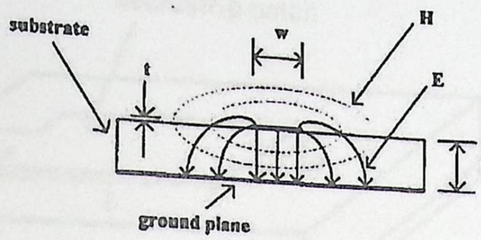

Figure 3.3.2: b. Electric field line

Hence, as shown in Figure 3.3.2, most of the electric field lines reside in the substrate and parts of lines exist in air. As a result this transmission line cannot support pure transverse electro-magnetic (TEM) mode of transmission, since the phase velocities would be different in the air and the substrate. Instead, the dominant mode of propagation is quasi-TEM mode. Hence, an effective dielectric constant must be obtained in order to account for the fringing and the wave propagation in the line The value of is slightly less than because the fringing fields around the periphery of the patch are not confined in the dielectric substrate but are also spread in the air as shown in Figure 3.3.2 above.[24]

The expression of effective dielectric constant is:

$$\varepsilon_{reff} = \frac{\varepsilon_r + 1}{2} + \frac{\varepsilon_r - 1}{2}\left(1 + 12\frac{h}{w}\right)^{-0.5} \tag{3.1}$$

Effective Length, Resonant Frequency and Effective Width

We can see, in Figure 3.4, a rectangular microstrip patch antenna of length L and width W resting on a substrate of height h. The coordinate axes is selected such that the length is along the x direction, width is along the y direction and the height is along the z direction.

In order to operate in the fundamental TM_010 mode, the length of the patch must be slightly less than $\lambda_g/2$ where λ_g is the wavelength in the dielectric medium and is equal to $\lambda_o/\sqrt{\varepsilon_{eff}}$ where λ_o is the free space wavelength. The TM_10 mode implies that the field varies one $\lambda_g/2$ cycle along the length, and there is no

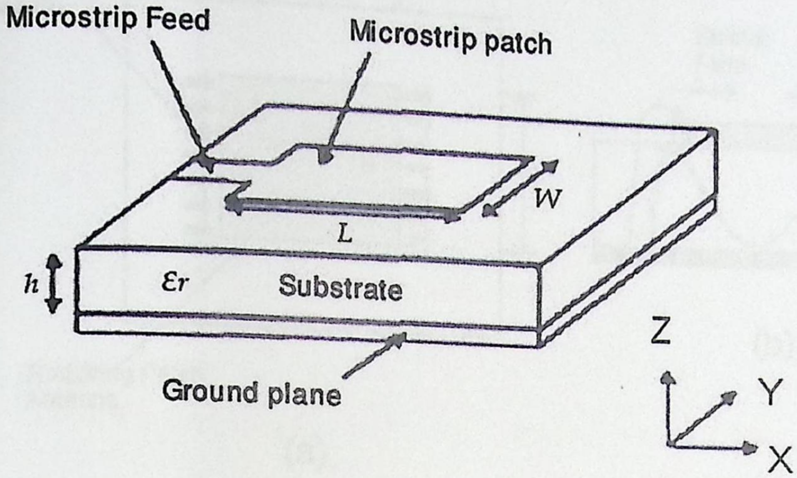

Figure 3.3.3: Rectangular microstrip patch antenna

variation along the width of the patch.

see Figure 3.3.1: a . The microstrip patch antenna is represented by two slots, separated by a transmission line of length L, and open circuited at both ends. Along edge of the patch, the voltage is maximum and current is minimum due to the open ends. The fields at edges can be resolved into normal and tangential components with respect to the ground plane

It is shown in Figure 3.3.2: b that the normal components of the electric field at the two edges along the width are in opposite directions and thus out of phase since the patch is $\lambda_g/2$ long and hence they cancel each other in the broadside direction. The tangential components, seen in Figure 3.5, which are in phase, means that the resulting fields combine to give maximum radiated field normal to the surface of the structure. Hence the edges along the width can be represented as two radiating slots, which are $\lambda_g/2$ apart and excited in phase and radiating in the half space above the ground plane. The fringing fields along the width can be modeled as radiating slots and electrically the patch of the microstrip antenna

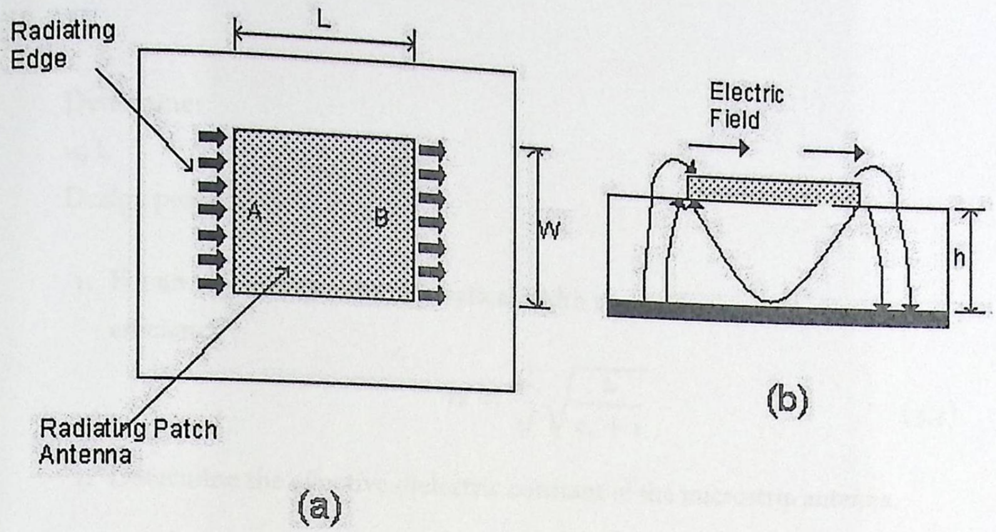

Figure 3.3.4: Physical and effective length of rectangular microstrip patch (a) Top view of the antenna (b) Side view of the antenna

looks greater than its physical dimensions. The dimensions of the patch along its length have now been extended on each end by a distance ΔL . This is given by:

$$\Delta L = 0.412h \frac{(\varepsilon_{reff} + 0.3)\left(\frac{w}{h} + 0.264\right)}{(\varepsilon_{reff} - 0.258)\left(\frac{w}{h} + 0.8\right)} \tag{3.2}$$

The effective length of the patch $_{eff}$ now becomes

$$L_{eff} = L + 2\Delta\, L \tag{3.3}$$

Design

Based on the simplified formulation that has been described a design procedure is outlined which leads to practical designs of rectangular microstrip antenna. The procedure assumes that the specified information includes the dielectric constant of the substrate ε_r , the resonant frequency f and the height of the substrate h. The procedure is as follows:[23]

Specify:

ε_r, f (in Hz), and h

Determine:

w, L

Design procedure:

1. For an efficient radiator, a practical width that leads to good radiation efficiency .

$$W = \frac{C}{2f}\sqrt{\frac{2}{\varepsilon_r + 1}} \tag{3.4}$$

2. Determine the effective dielectric constant of the microstrip antenna.

3. Once W is found determine the extension of the length ΔL.

4. The actual length of the patch can now be determined by.

$$L = \frac{C}{2f\sqrt{\varepsilon_{eff}}} - 2\Delta L \tag{3.5}$$

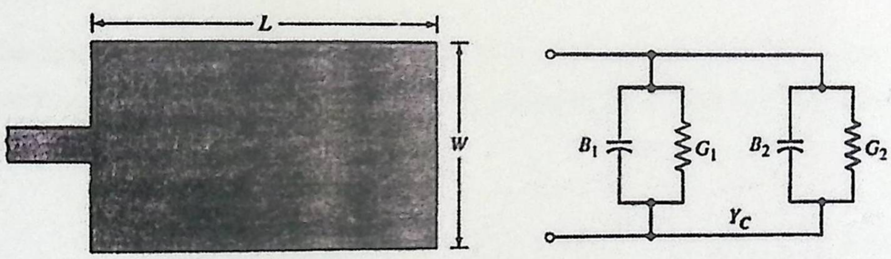

Figure 3.3.5: Rectangular microstrip patch and its equivalent circuit transmission model

Transmission Line

The width of 50 Ω transmission line is,

$$\frac{w}{h} = \frac{2}{\pi}\{B - 1 - ln(2B - 1) + \frac{\varepsilon_r - 1}{2\varepsilon_r}[ln(B - 1) + 0.39\frac{0.61}{\varepsilon_r}] \tag{3.6}$$

$$B = 60\,\frac{\pi^2}{Z_0\,\varepsilon_r}$$

We choose the length of transmission line so suitable to our design.

Qwadrature wave length(QWL)

The length of QWL is given by,

$$L(QWL) = \frac{\lambda}{4 * \sqrt{\varepsilon_r}} \tag{3.7}$$

$$\frac{w}{h} = \frac{8\,\exp(A)}{\exp(2\,A) - 2} \tag{3.8}$$

Where A, The width of QWL is obtained from this equation.

$$A = \frac{Z_0}{60}\left(\frac{\varepsilon_r + 1}{2}\right)^{1/2} + \frac{\varepsilon_r - 1}{\varepsilon_r + 1}\left(0.23 + \frac{0.11}{\varepsilon_r}\right) \tag{3.9}$$

Ground Plane

The dimensions of the ground plane were taken according to the length of the patch, quarter wave transformer and the 50 Ω transmission line. So the length of the ground plane will be given by;

$$L_g = L + LQWL + LTL \tag{3.10}$$

Where L is the length of the patch, LQWT is the length of the quarter wave transformer; LTL is the length of the 50 Ω transmission line. The ground plane is made of copper sheet; the thickness of copper sheet is taken to be 0.1 mm.[25]

Dielectric

FR4 ($\varepsilon_r = 4.4$) dielectric material used,

Length= length of the ground.

Width =width of the ground.
Thickness (h) =1.6mm.

3.4 Experiments for the project

To ensure the value of the dielectric constant or relative permittivity for dielectric material (because we don't have a device 85070E Dielectric Probe Kit figure 3.3 that used to determines the intrinsic electromagnetic properties of many dielectric materials) that will be used as a skin phantom in this project we doing the following experiments :

We measure the capacitance value for plate of glass as a reference value with 11.5cm length,4.5cm width and 2.5mm highest by capacity meter device this giving us 0.077nf

By using the following equation we calculate the dielectric constant

$$C = \frac{\varepsilon_o \varepsilon_r A}{d} \tag{3.11}$$

Where :

C :capacitance

ε_o = dielectric constant of air ($8.85 * 10^{-}12$)

ε_r = dielectric constant of material (glass material)

A :area of plate

d: highest of plate

we find the dielectric constant equal to 4.2 and this value lie in the range of glass(3.8:14.5)

to find the conductivity according to the following equation

$$R = \frac{d}{\sigma_A} \tag{3.12}$$

Where

R = resistance value (Ω)

σ = Conductivity

We use the meggure device to measure the resistance value of glass that equal to 500 MΩ

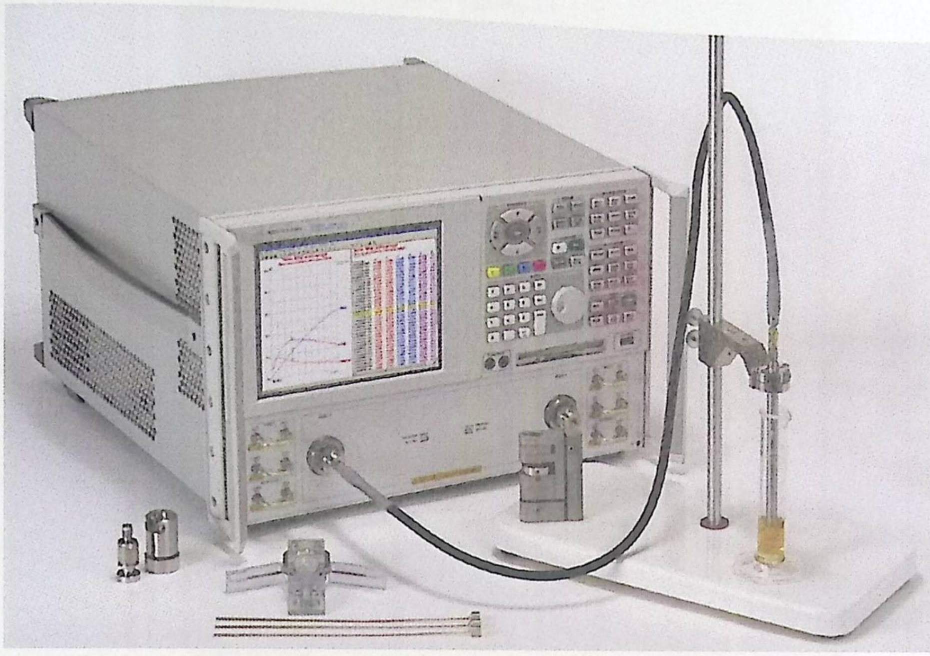

Figure 3.4.1: Dielectric probe kit.

Take risk, if you win, you will be happy, if you lose you will be wise.

Peter Kreeft

4 Microstrip Patch Antenna Design and Results

4.1 Design Features

The ability of the design for microstrip antenna to using in breast cancer detection come from adding a matching stub at the input port, and moving the feed port towards the edge to increase the impedance of the antenna.

The optimization is performed for the design. The size of the microstrip patch (length and width), and the size and position of the feed and stub is changed during the optimization. The reflection coefficients and input impedances of the optimized antennas to be used in contact with the skin are presented.

4.2 Calculations of skin impedance.

Because there is no device available to measure the impedance, permeability and conductivity of the skin at 2.45GHz we use a published curves are showing in figure 4.2.1 and 4.2.2 as a reference to find the permittivity and conductivity respectively for tumor and tumor median, skin and skin median.

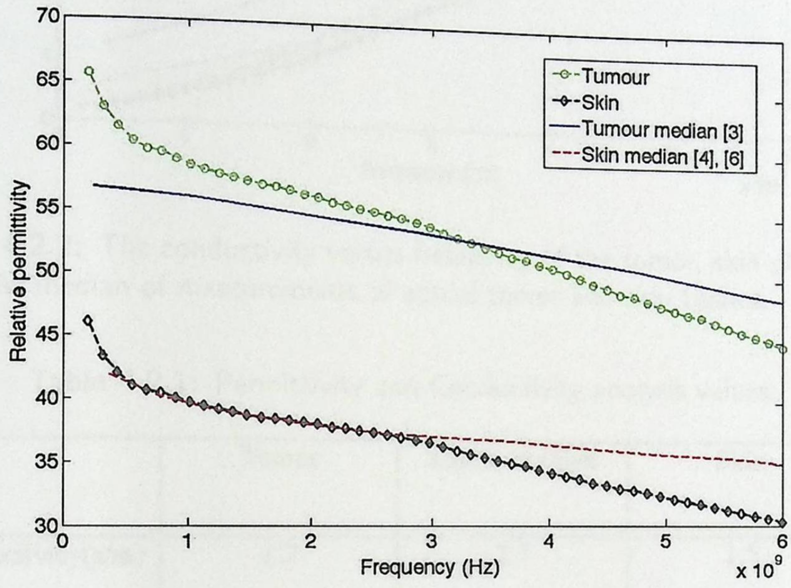

Figure 4.2.1: The permittivity versus frequency for skin and tumor phantoms as well as the median from measurements of actual skin tissue and actual malignant tissue.

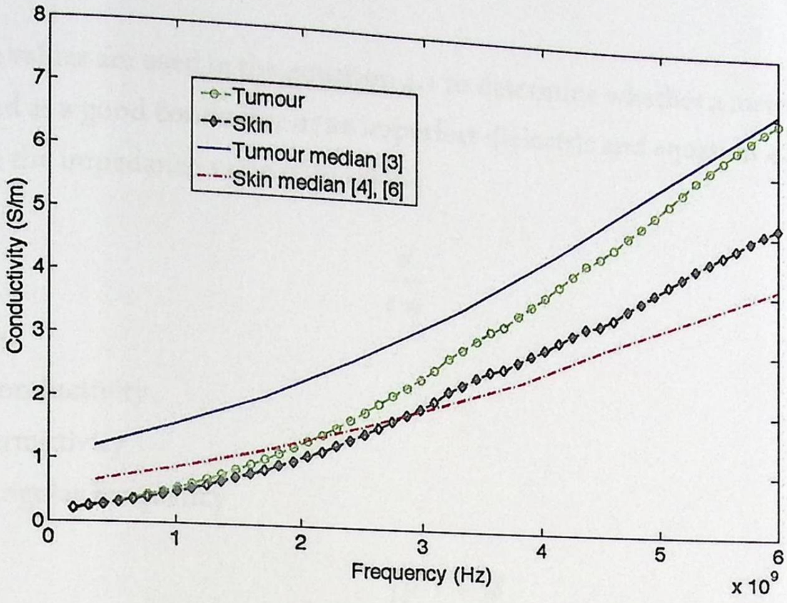

Figure 4.2.2: The conductivity versus frequency of the tumor, skin phantoms, the median of measurements of actual tumor and skin tissues.

Table 4.2.1: Permittivity and Conductivity analysis values.

	Tumor	Tumor median	Skin	Skin Median
Conductivity(s/m)	1.7	2.7	1.5	1.6
Permittivity	51	54	37.5	37.5

These values are used in the equation 4.1 to determine whether a material can be classed as a good conductor or an imperfect dielectric and equation 4.2 to calculate the impedance value of the skin :

$$\frac{\sigma}{\varepsilon\, w} \tag{4.1}$$

Where

σ = Conductivity

ε = Permittivity

w = Angular Frequency

$$\eta_c = \sqrt{\frac{\mu}{\varepsilon}\,\frac{1+j\delta}{2\varepsilon w}} \tag{4.2}$$

Where

η_c = Intrinsic impedance

μ = Permeability

ε = Permittivity

δ = loss angle

w = Angular Frequency

Table 4.2.2: The impedance values according to the previous analysis.

	Skin	Skin median	Tumor	Tumor Median
Impedance	37.5	62.31	53.19	52.157

4.3 Design of rectangular Patch Microstrip Antenna for breast cancer detection using HFSS Simulator.

4.3.1 Design where the Stub at the Center of the patch.

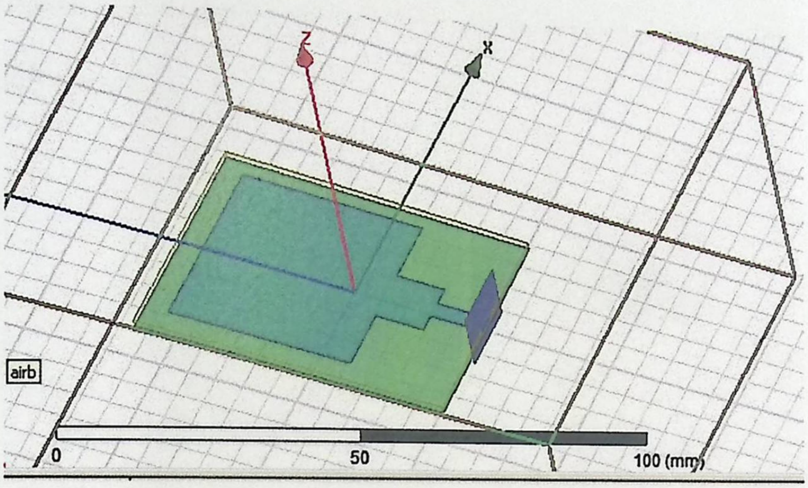

Figure 4.3.1: Design of the patch where the stub at the center without existing skin.

The analysis results for this design in figures 5.2.3, 4.3.3 and 4.3.4

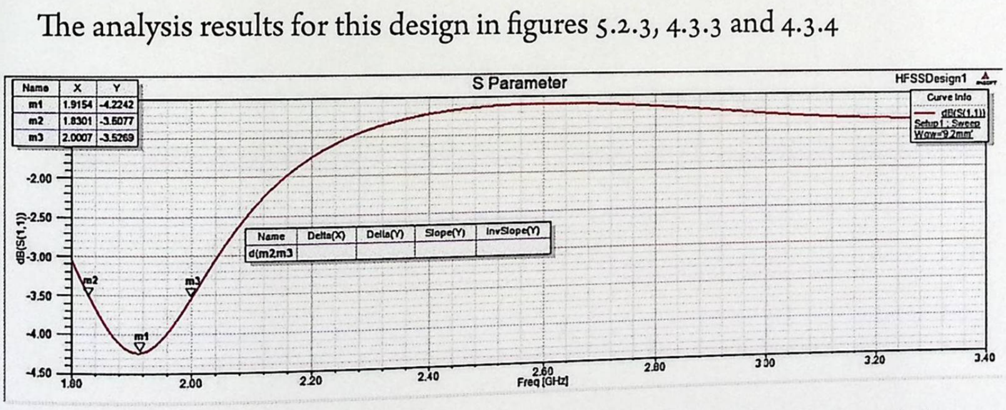

Figure 4.3.2: Return loss vs. frequency for antenna patch without existing skin.

- Return loss = - 4.2242 dB

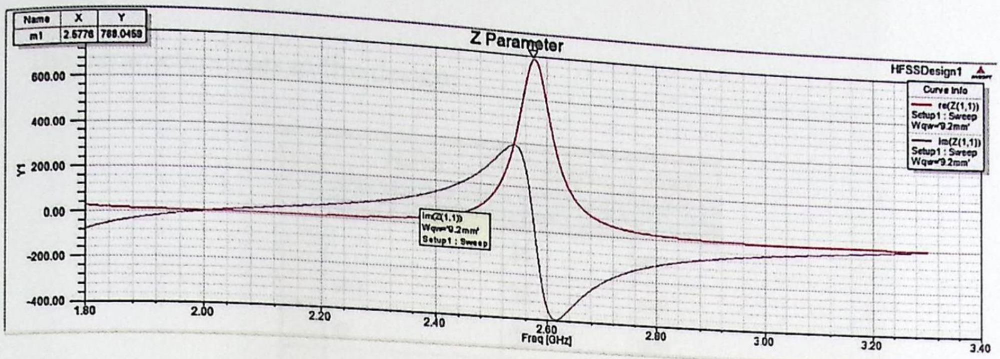

Figure 4.3.3: Input impedance curve for antenna patch without existing skin.

- re(Z) = 788 Ω

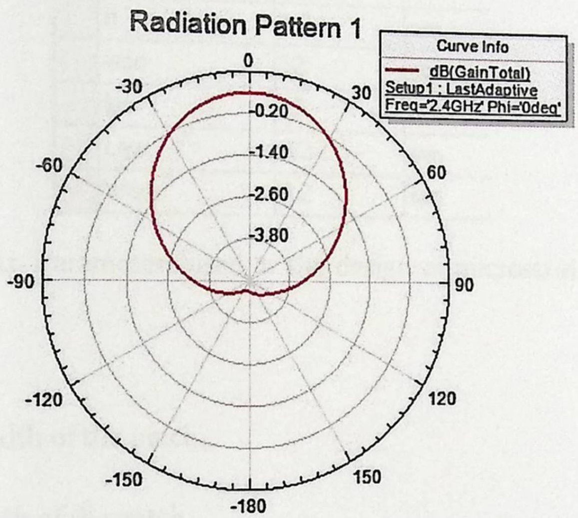

Figure 4.3.4: Radiation Pattern for antenna patch without existing skin.

The parameters uses in the design:

Name	Value	Unit
w	31	mm
l	34	mm
wg	38	mm
lg	58	mm
wd	38	mm
ld	58	mm
wt	2.915	mm
lt	10	mm
t	0.1	mm
h	1.6	mm
wpo	12	mm
lpo	12	mm
Lqw	9.2	mm
Wqw	9.2	mm

Figure 4.4.1: Parameters used in the design of microstrip antenna.

Where:

- W: is the width of the patch.
- l: is the length of the patch.
- Wg: is the width of the ground box.
- lg: is the length of the ground box.
- wd: is the width of the dielectric (FR4).
- ld: is the length of the dielectric(FR4).
- wt : the width of the transmission line.
- lt : is the length of the transmission line.

- t : is the height of the ground.
- h :is the height of dielectric.
- wpo: is the width of the port.
- lpo : is the length of the port.
- Lqw:is the length of the stup.
- Wqw: is the width of the stup.

After we added a normal skin layer for this design as in figure 4.3.5

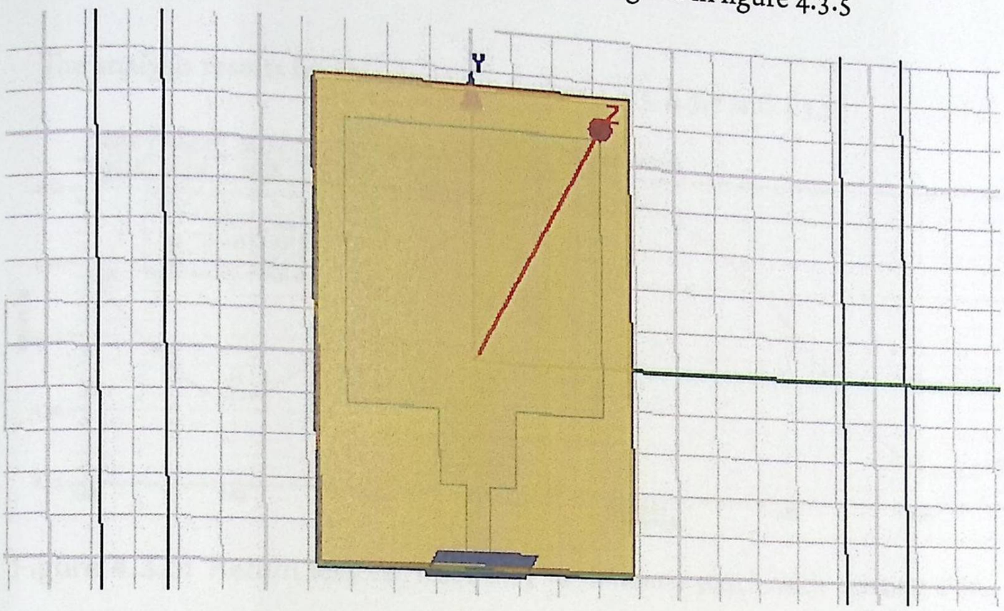

Figure 4.3.5: Design of the patch where the stub at the center with existing skin.

The analysis results for this design in figures 5.2.5, 4.3.7 and 4.3.8

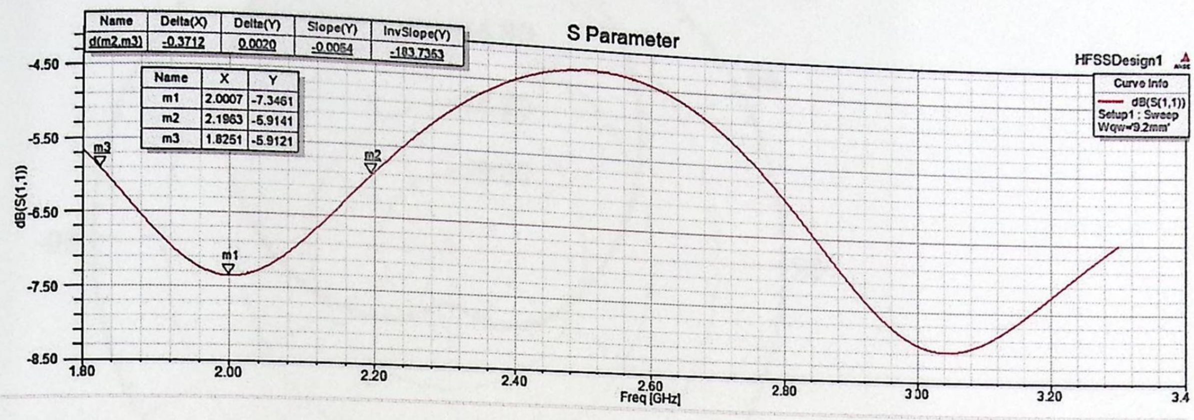

Figure 4.3.6: Return loss vs. frequency for antenna patch with existing skin.

- Return loss = - 7.3461 dB

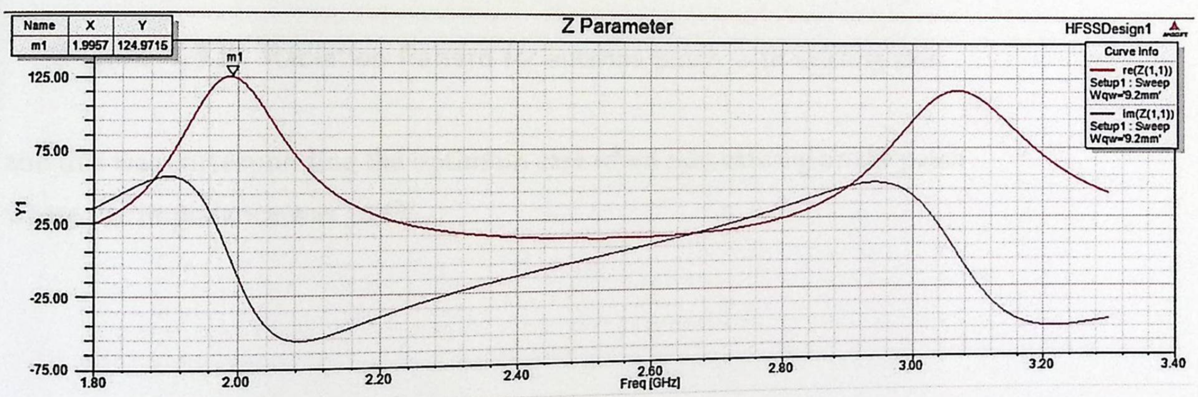

Figure 4.3.7: Input impedance curve for antenna patch with existing skin.

- re(Z) = 124.97 Ω

We get results in the tables below after we moved the stub several steps toward the edge until reached 620 Ω impedance of the patch only without existing skin

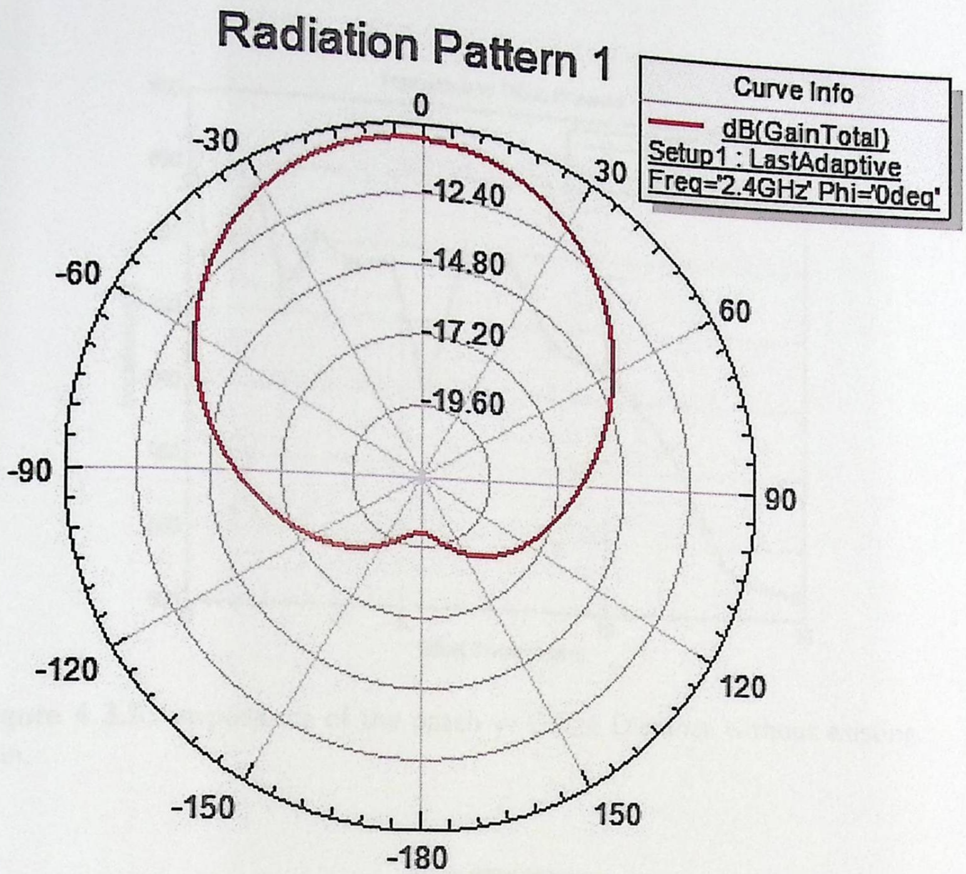

Figure 4.3.8: Radiation Pattern for antenna patch with existing skin.

and this was corresponding the optimum case when skin existing on the patch where the impedance was 50 Ω.

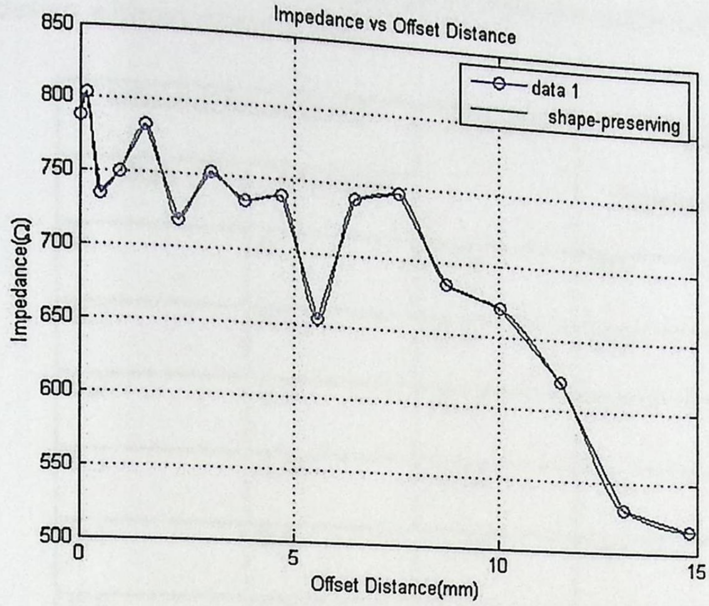

Figure 4.3.9: Impedance of the patch vs Offset Distance without existing skin.

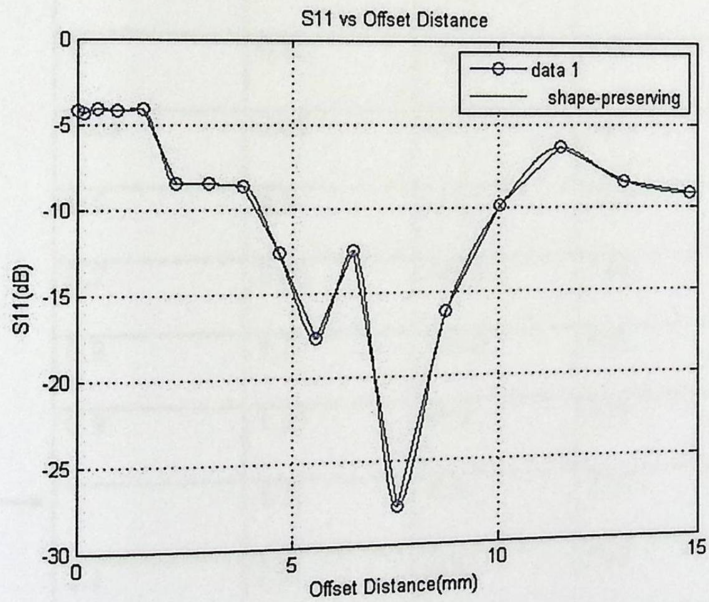

Figure 4.3.10: Return loss of the patch vs Offset Distance without existing skin.

Table 4.3.1: The analysis values of the patch from the center until reach optimum design without existing skin.

Offset distance (mm)		S11(dB)	Real Impedance(Ω)
Stub	Feed line		
0	0	4.22-	788
0.1	0.15	-4.3	803
0.2	0.3	-4.12	735
0.3	0.45	-4.22	750
0.4	0.6	-4.14	783
0.5	0.75	-8.5	719
0.52	0.77	-8.54	752
0.55	0.8	-8.69	734
0.6	0.85	-12.6	739
0.63	0.88	-17.7	655
0.6	0.9	-12.5	740
0.7	1.05	-27.8	746
0.8	1.2	-16.2	685
0.9	1.35	-9.9	670
→ 1	1.5	6.4-	620
1.1	1.6	8.5-	530
1.2	1.65	-9.2	516

The Arrow indicates to the optimum design without existing skin.

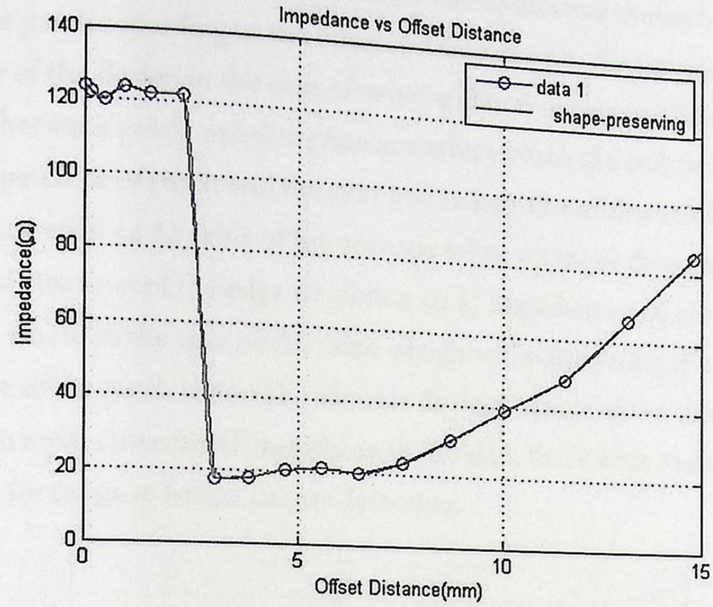

Figure 4.3.11: Impedance of the patch vs Offset Distance with existing skin.

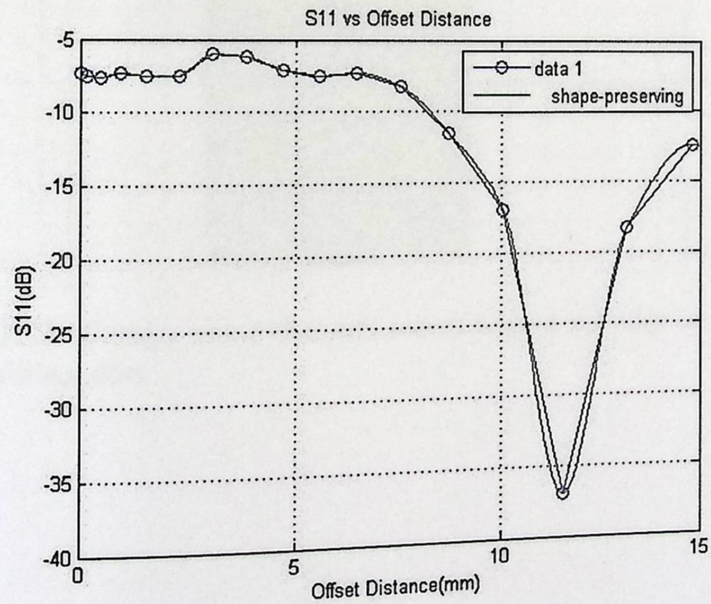

Figure 4.3.12: Return loss of the patch vs Offset Distance with existing skin.

4.3.2 Design where the Stub moves toward the edge of the patch.

Optimal patch design where the stub and transmission line moves toward the edge of the patch according to the offset distance steps in the previous tables, the optimality of the design in the case of existing skin is occurring the impedance matching between patch and skin phantom where when the stub at the center the overall impedance of patch and the skin was 124.97 Ω and this will lead mismatching with 50 Ω cable of the antenna when we move this stub far away from the center toward the edge we obtain 50 Ω impedance and get the matching, where in the case of the same design without existing skin the impedance of the patch is 620 Ω , whereas the impedance of the skin is 62.31 Ω that's mean most current will pass through the skin, that's what make the design applicable for usage in breast cancer detection.

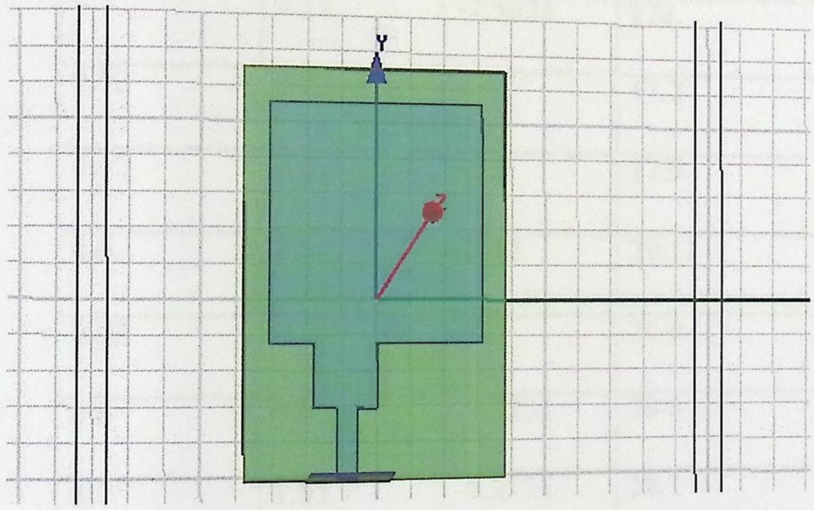

Figure 4.3.13: Design where the stub moves toward the edge of the patch without existing skin.

Table 4.3.2: The analysis values of the patch from the center until reach optimum design with existing skin.

Offset distance (mm)		S11(dB)	Real Impedance(Ω)
Stub	Feed line		
0	0	-7.3461	124.97
0.1	0.15	-7.556	122
0.2	0.3	-7.6764	120.44
0.3	0.45	-7.373	124
0.4	0.6	-7.5238	122.4
0.5	0.75	-7.5621	122
0.52	0.77	-6	17.2
0.55	0.8	-6.2	17.9
0.6	0.85	-7.12	20.11
0.63	0.88	-7.5	20.9
0.6	0.9	-7.3251	20.8
0.7	1.05	-8.2732	23.1
0.8	1.2	-11.5473	30.14
0.9	1.35	-16.9158	39
→ 1	1.5	-37.09	48.7
1.1	1.6	-18.31	66.26
1.2	1.65	-12.41	85.46

The Arrow indicates to the optimum design with existing skin.

The analysis results for this design in figures 5.2.7, 4.3.15 and ??

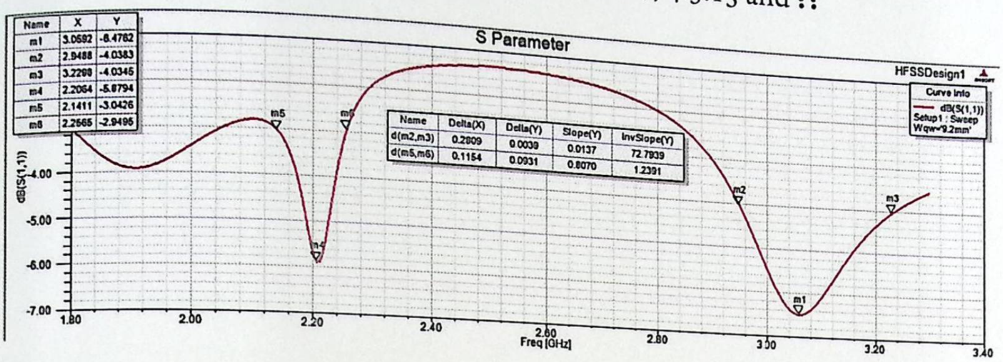

Figure 4.3.14: Return loss vs. frequency for antenna patch without existing skin.

- Return loss = - 5.87 dB

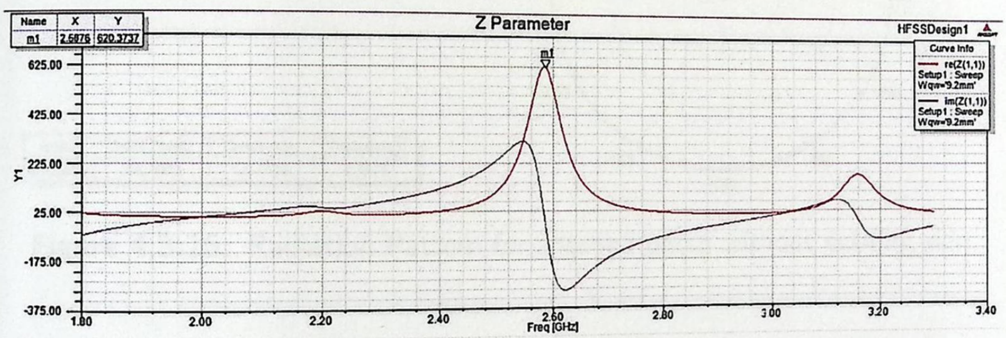

Figure 4.3.15: Input impedance curve for antenna patch without existing skin.

- re(Z) = 620.37 Ω

Name	Theta	Ang	Mag
m1	0.0000	0.0000	0.7787
m2	-65.0000	-65.0000	-2.7713
m3	68.0000	68.0000	-2.2705

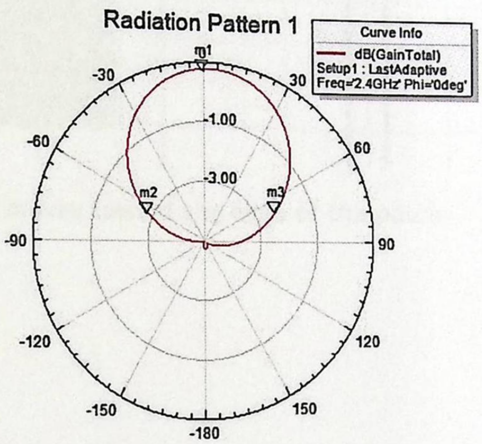

Name	Delta(Theta)	Delta(Ang)	Delta(Mag)
d(m2,m3)	133.0000	133.0000	0.5009

Figure 4.3.16: Radiation Pattern for antenna patch without existing skin.

After we added a normal skin layer for this design as in figure 4.3.19

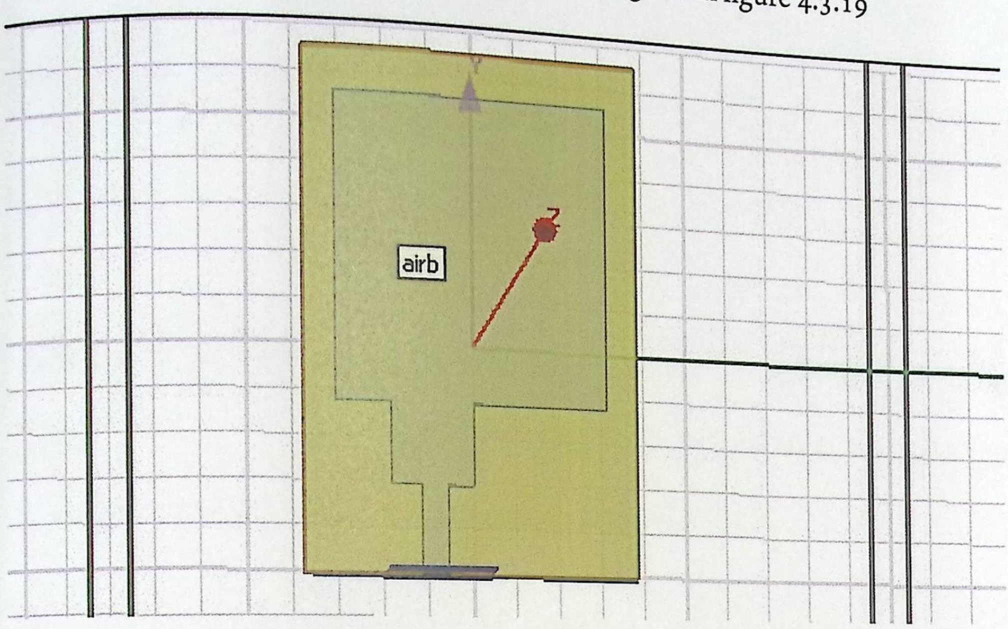

Figure 4.3.17: Design where the stub moves toward the edge of the patch with existing skin.

The analysis results for this design in figures 5.2.9, 4.3.19 and ??

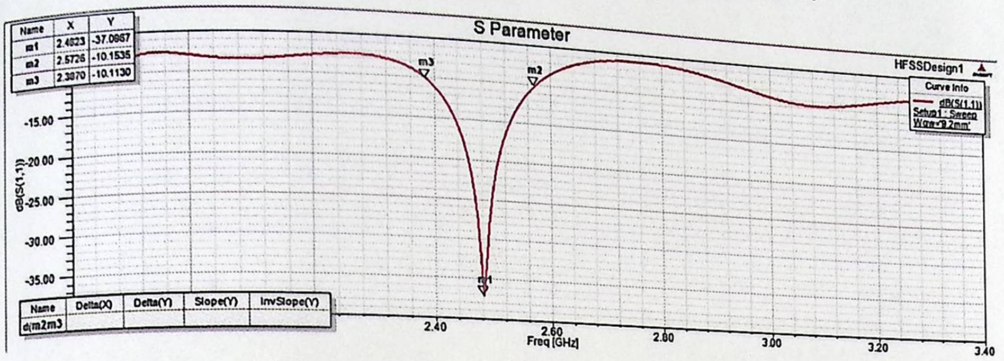

Figure 4.3.18: Return loss vs. frequency for antenna patch with existing skin.

- Return loss = - 37 dB,   bandwidth = 185.6 MHz.

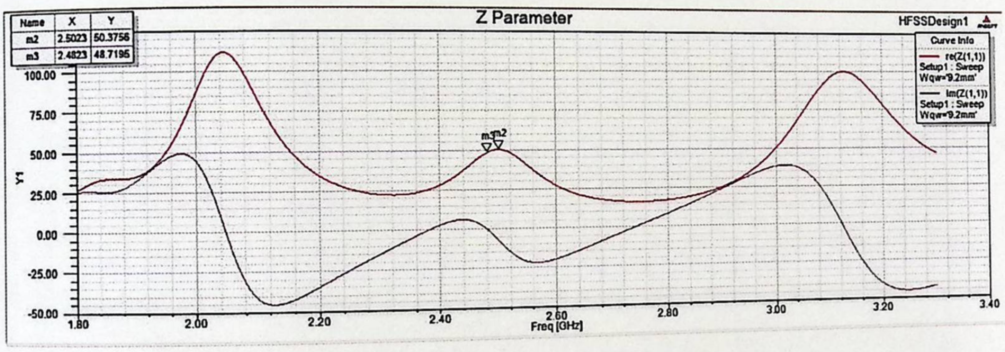

Figure 4.3.19: Input impedance curve for antenna patch with existing skin.

- re(Z) = 48.7 Ω

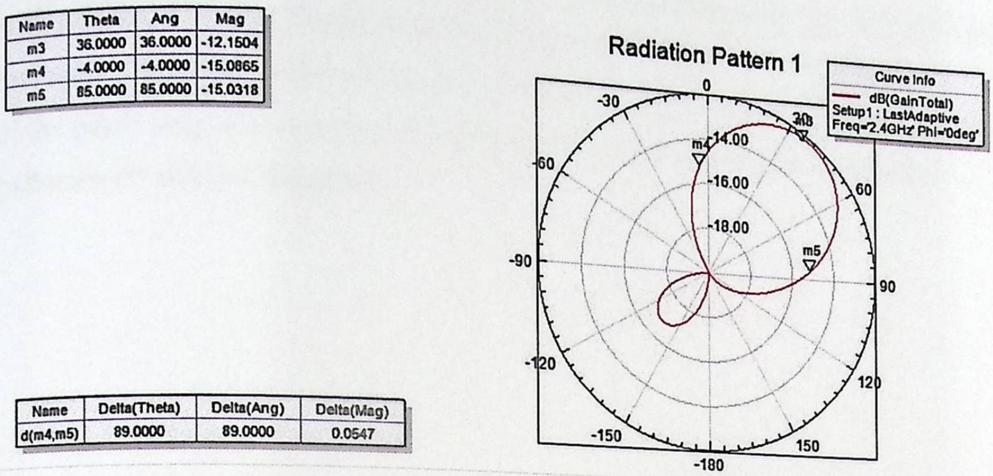

Name	Theta	Ang	Mag
m3	36.0000	36.0000	-12.1504
m4	-4.0000	-4.0000	-15.0865
m5	85.0000	85.0000	-15.0318

Name	Delta(Theta)	Delta(Ang)	Delta(Mag)
d(m4,m5)	89.0000	89.0000	0.0547

Figure 4.3.20: Radiation Pattern for antenna patch with existing skin.

4.4 Conclusion

By simulation observing, movement of the stub lead to obtain impedance matching between patch and the skin phantom where when the stub at the center the overall impedance of patch and the skin was 124.97 Ω and this will lead mismatching with 50 Ω cable of the antenna when we move this stub far away from the center toward the edge we obtain 50 Ω impedance and get the matching. We get this result after we moved the stub several steps toward the edge until reached 50 Ω impedance and this was the optimum case. At the optimum design we find that the overall impedance is 50 Ω ,where the impedance of the patch only when eliminating the skin is 620 Ω , whereas the impedance of the skin is 62.31 Ω that's mean most current will pass through the skin, that's what make the design applicable for usage in breast cancer detection.

According to return loss carves we observed that the best value of S11 parameter obtained by the optimum case it was - 37 dB where in the other cases it was less than – 10 dB that's mean the antennas not working .

Referring to the radiation pattern plots in figures 4.3.18, 4.3.22, we can say that the radiation pattern in the case of existing skin with a patch of antenna is differ than the case with no skin on the patch, the gain with skin is greater than the gain with no skin, although attenuation occurred with adding skin, so the gain increases due to the radiation pattern with skin has more directivity than the case of the patch only without skin and this will lead to obtain improved radiation pattern with skin on the patch.

One thing I have learned in a long life : that all our science, measured against reality, is primitive and childlike – and yet is the most precious thing we have .

Albert Einstin

5

Antenna Measurement Results

5.1 Overview

In this chapter we will introduce our measured results of the return loss and radiation pattern for rectangular patch microstrip antennas operates at 2.45 GHz.

These antennas were fabricated using FR4 substrate with thickness 1.6 mm using PCB prototype machine to use it for detection of breast cancer.

5.2 Measurements of rectangular Patch Microstrip Antenna.

We measured the rerun loss of the rectangular patch microstip antenna using Site Master system at al-wataniya mobile company because this system not available in our university.

The system was first calibrate for open circuit load, short circuit load and matched load 50 ohm in order to establish the required reference points for the frequency range required. After that the microstrip antenna was connected to the Site Master via an SMA/N1 connector. We got the following measurements of reflection coefficient as shown in Figures below and it validated by simulations. The measured impedance bandwidth of the antenna is about 1600 MHz from1.8 to 3.4 GHz. A prototype of the proposed antennas is shown in figures 5.2.1 and 5.2.2 .

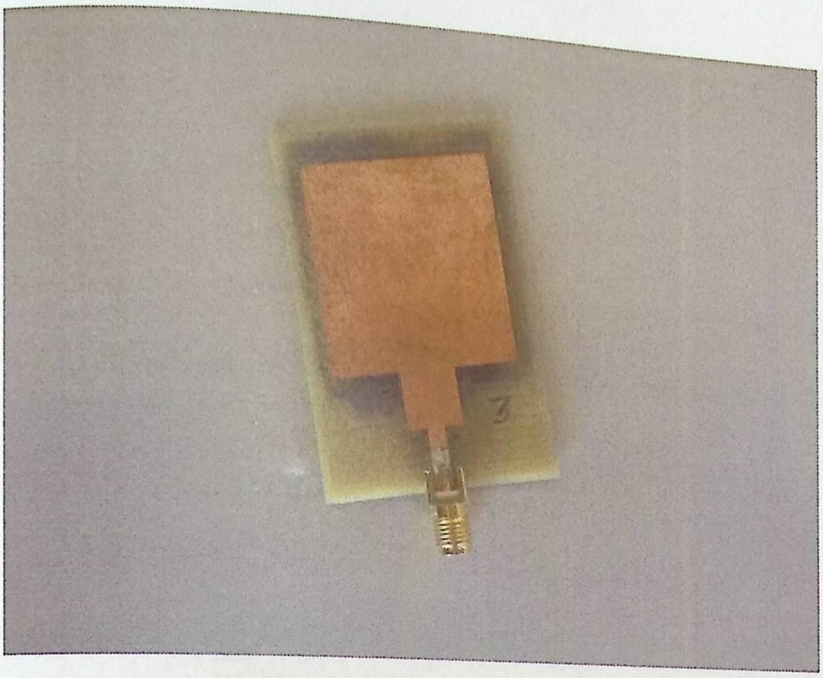

Figure 5.2.1: A prototype for antenna of center feed and stub position.

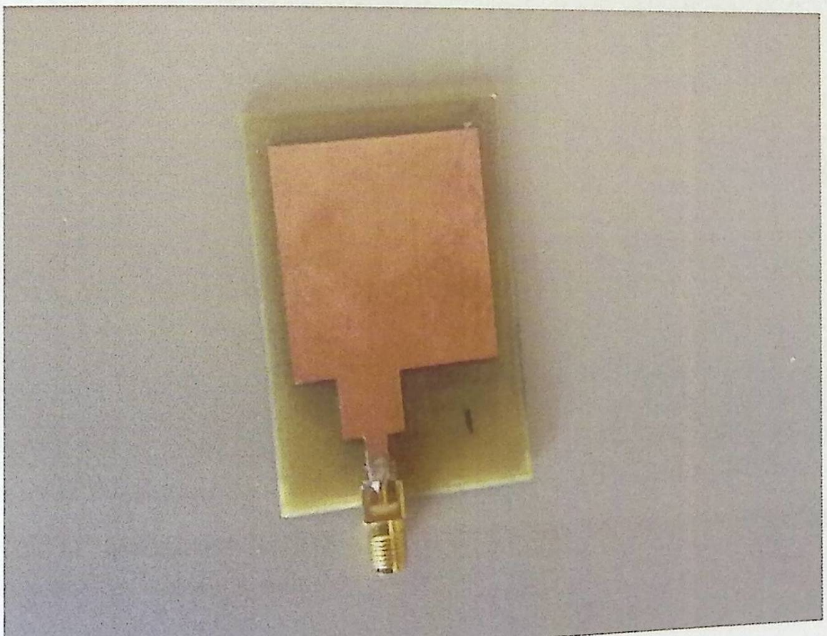

Figure 5.2.2: A prototype for optimum antenna which the feed and stub position shifted to the edge of patch.

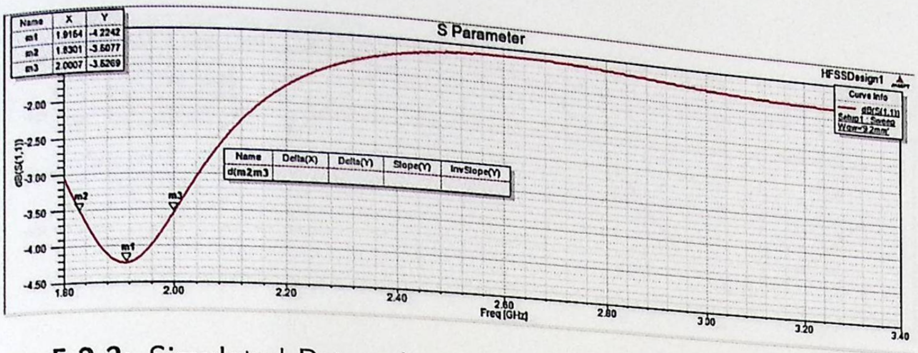

Figure 5.2.3: Simulated Return loss vs. frequency for antenna of center feed and stub position without existing skin.

- Return loss = - 4.2242 dB

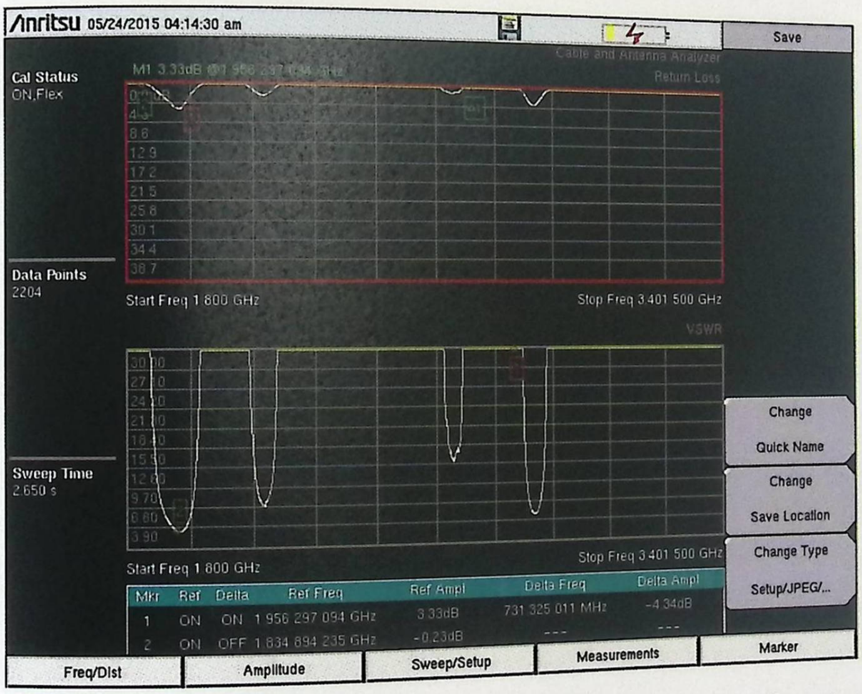

Figure 5.2.4: Measured Return loss vs. frequency for antenna of center feed and stub position without existing skin.

- Return loss = - 4.34 dB

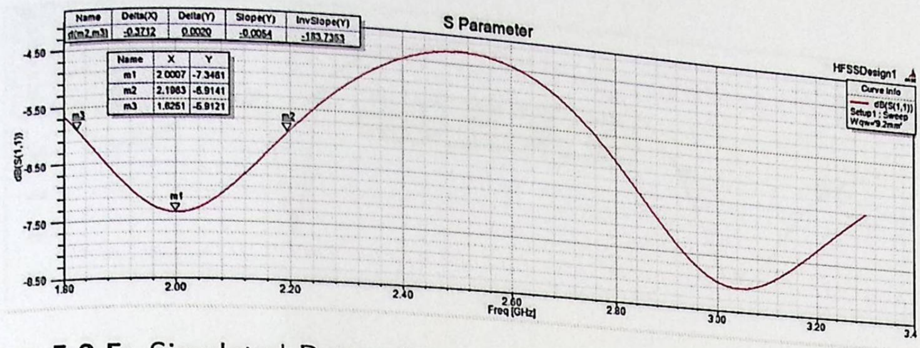

Figure 5.2.5: Simulated Return loss vs. frequency for antenna of center feed and stub position with existing skin.

- Return loss = - 7.3461 dB

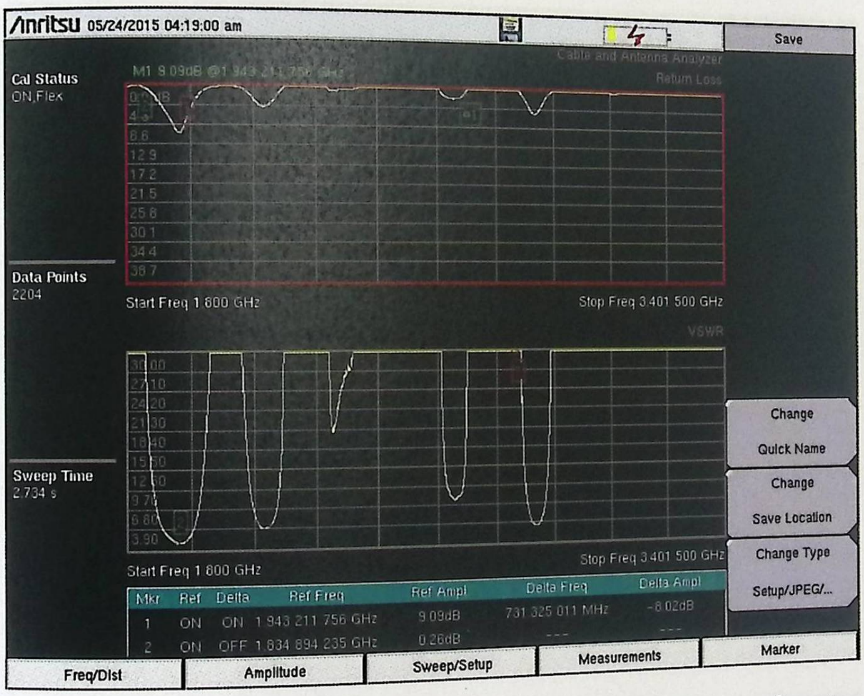

Figure 5.2.6: Measured Return loss vs. frequency for antenna of center feed and stub position with existing skin.

- Return loss = - 8.02 dB

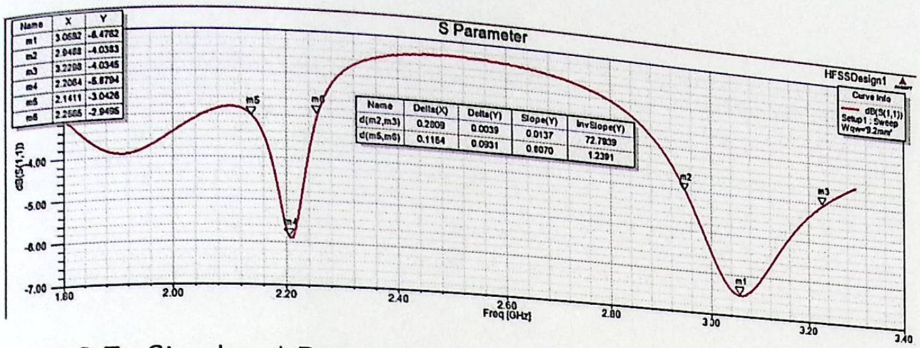

Figure 5.2.7: Simulated Return loss vs. frequency of Optimum antenna without existing skin.

- Return loss = - 5.87 dB

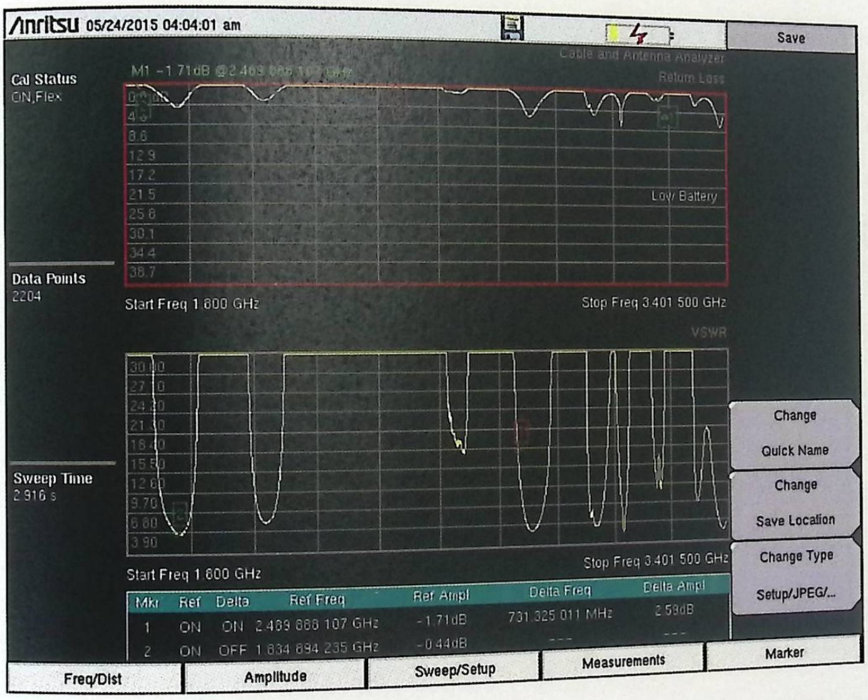

Figure 5.2.8: Measured Return loss vs. frequency of Optimum antenna without existing skin.

- Return loss = - 1.71 dB

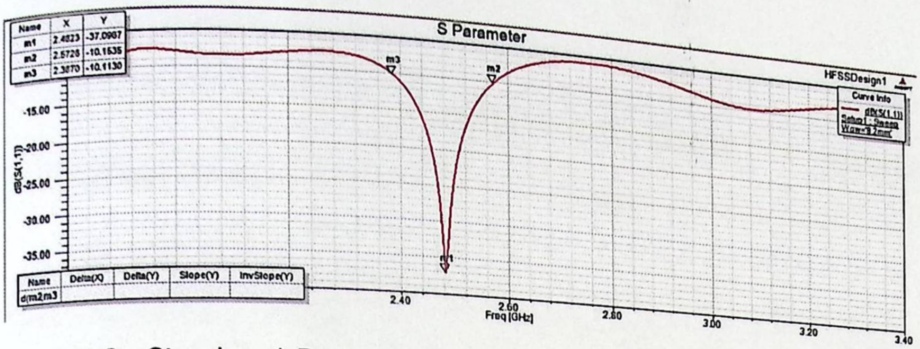

Figure 5.2.9: Simulated Return loss vs. frequency of Optimum antenna with existing skin.

- Return loss = - 37 dB

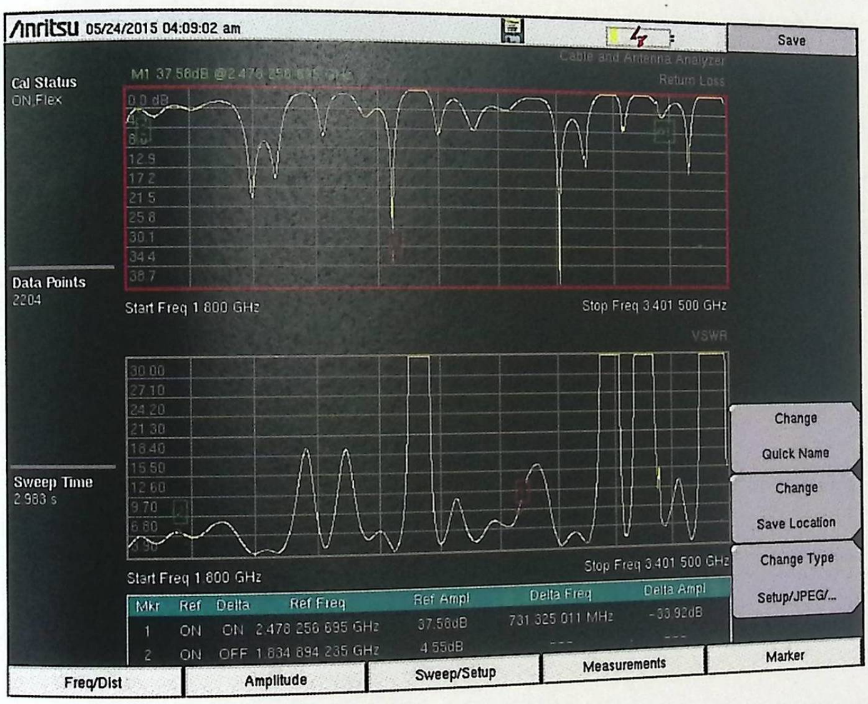

Figure 5.2.10: Measured Return loss vs. frequency of Optimum antenna with existing skin.

- Return loss = - 37 .58 dB

Table 5.2.1: Comparison between simulated and measured return loss values.

	Simulated Return loss S_{11}	Measured Return loss S_{11}
Optimum antenna with existing skin	- 37 dB	- 37 .58 dB
Optimum antenna without existing skin	- 5.87 dB	- 1.71 dB
Central antenna with existing skin	- 7.3461 dB	- 8.02 dB
Central antenna without existing skin	- 4.2242 dB	- 4.34 dB

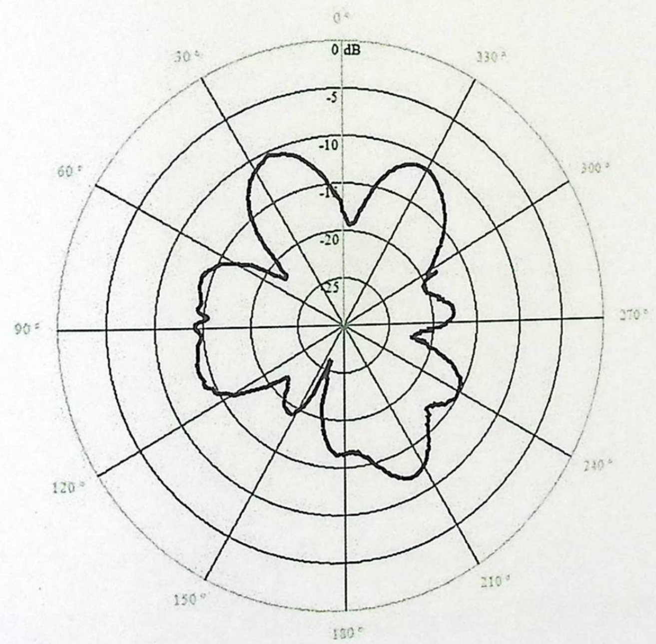

Figure 5.2.11: Measured E-plane Radiation Pattern of Optimum antenna on air.

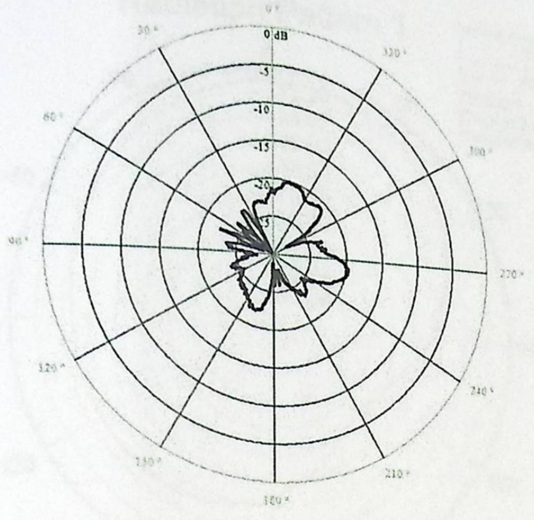

Figure 5.2.12: Measured E-plane radiation pattern of Optimum antenna with normal skin on Rx only.

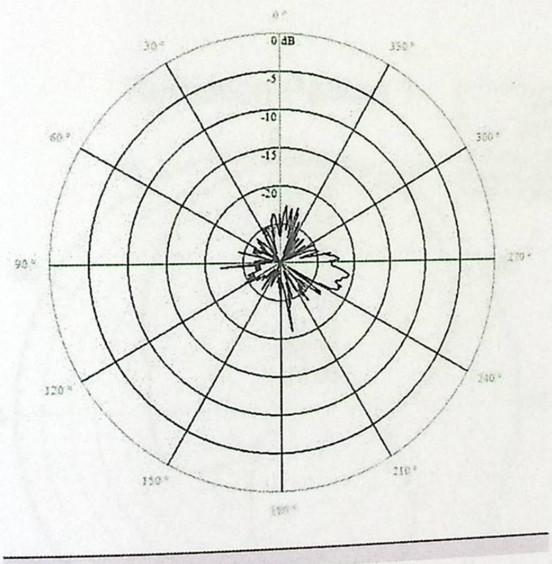

Figure 5.2.13: Measured E-plane radiation pattern of Optimum antenna with skin and tumor on Rx only.

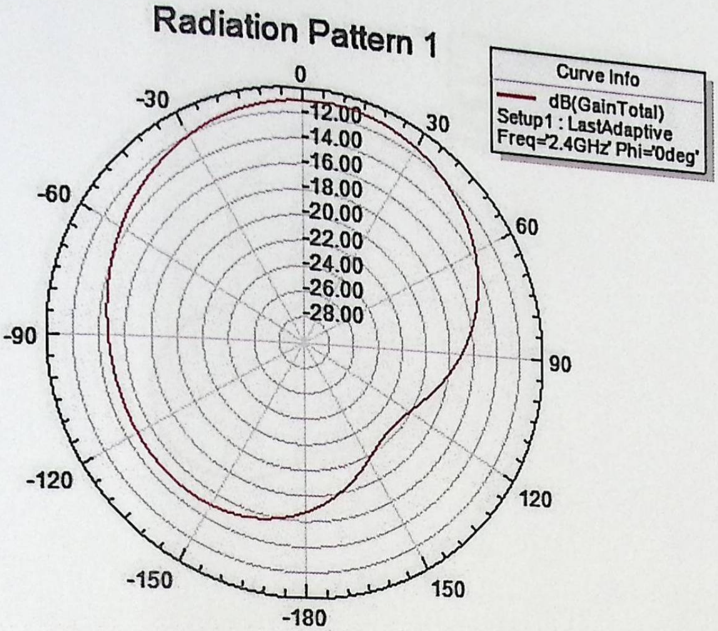

Figure 5.2.14: Simulated H-plane radiation pattern of Optimum antenna with tumor.

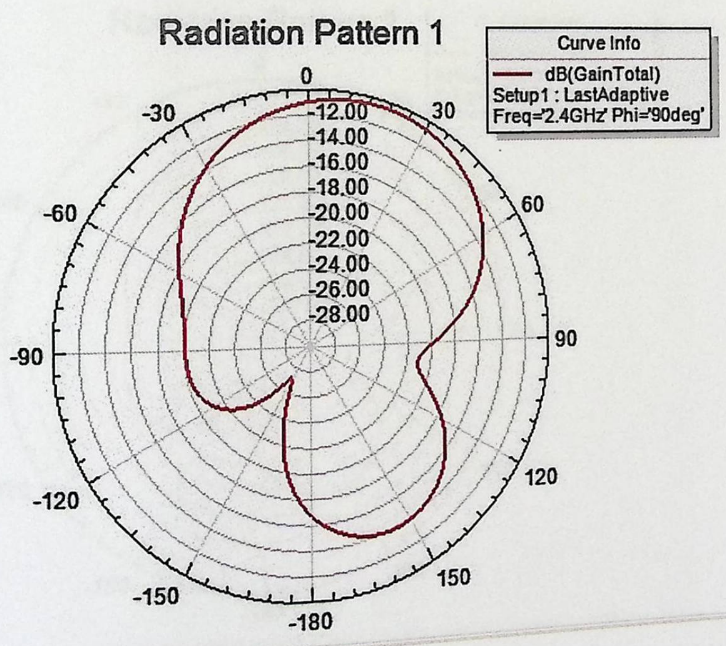

Figure 5.2.15: Simulated E-plane radiation pattern of Optimum antenna with tumor.

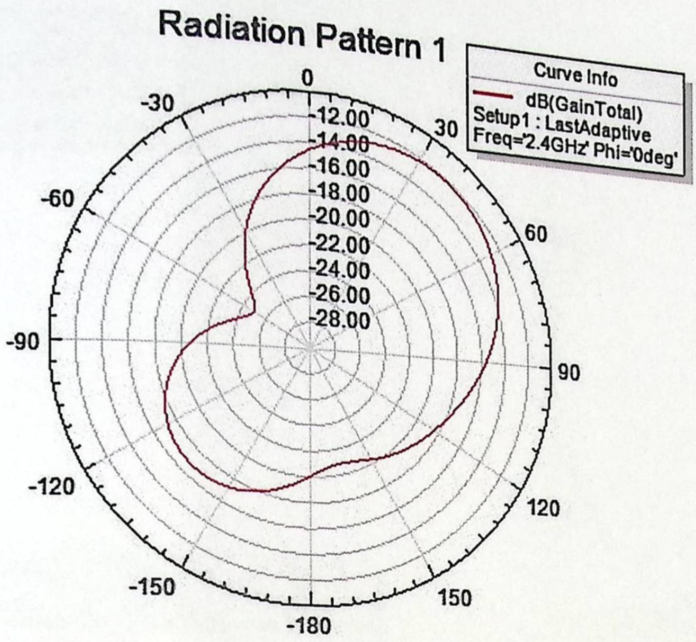

Figure 5.2.16: Simulated H-plane radiation pattern of Optimum antenna with normal skin.

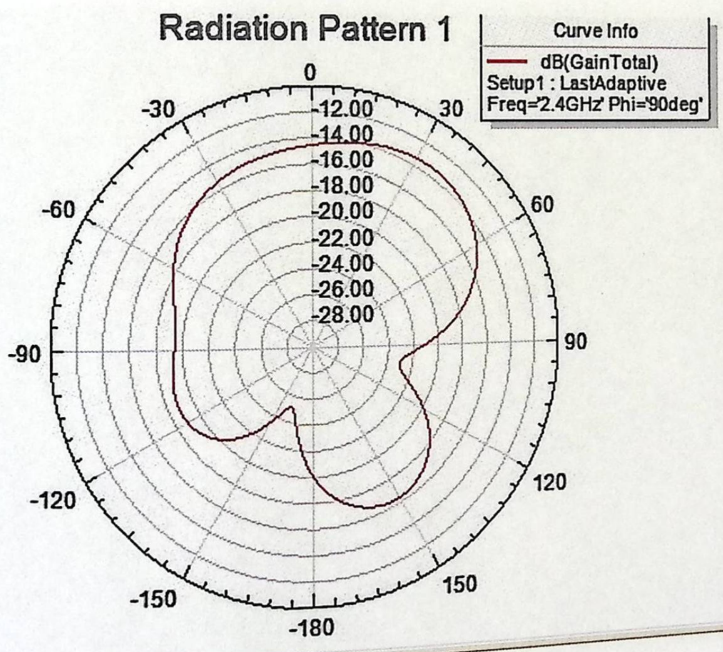

Figure 5.2.17: Simulated E-plane radiation pattern of Optimum antenna with normal skin.

Name	Theta	Ang	Mag
m3	36.0000	36.0000	-12.1504
m4	-4.0000	-4.0000	-15.0865
m5	85.0000	85.0000	-15.0318

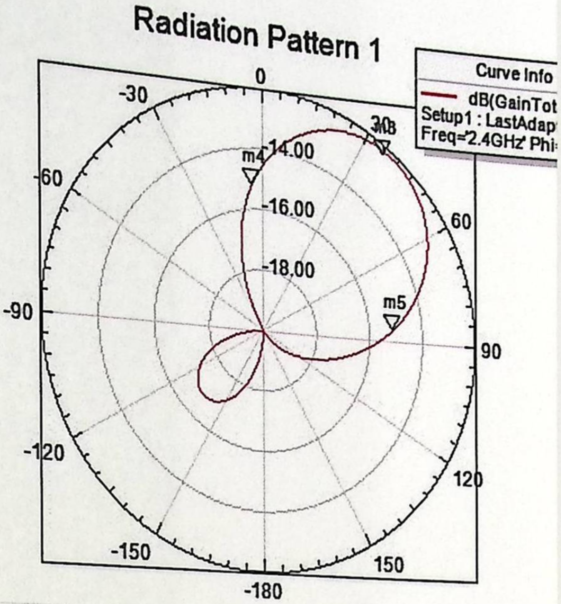

Name	Delta(Theta)	Delta(Ang)	Delta(Mag)
d(m4,m5)	89.0000	89.0000	0.0547

Figure 5.2.18: Simulated radiation pattern of Optimum antenna with normal skin.

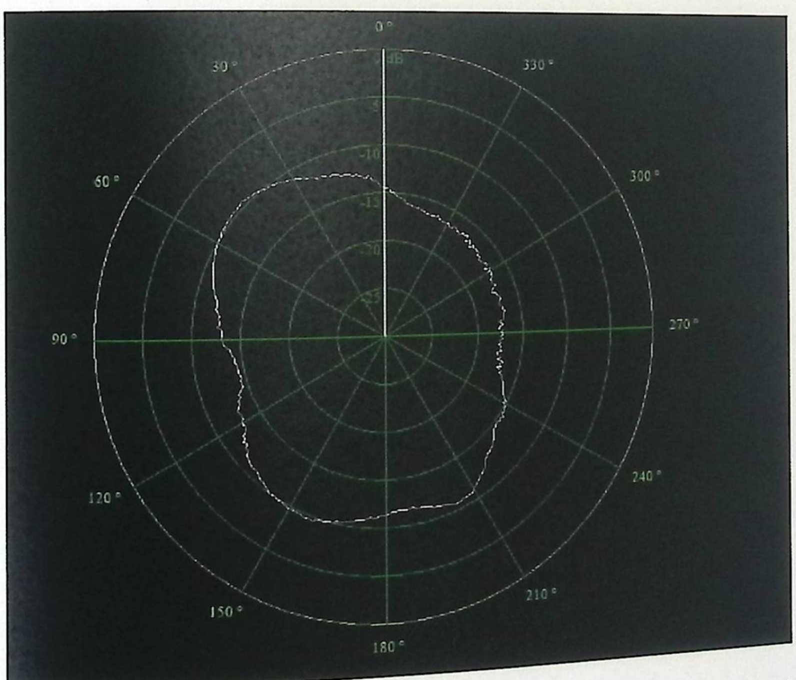

Figure 5.2.19: Measured H-Plane radiation pattern of Optimum antenna on Air.

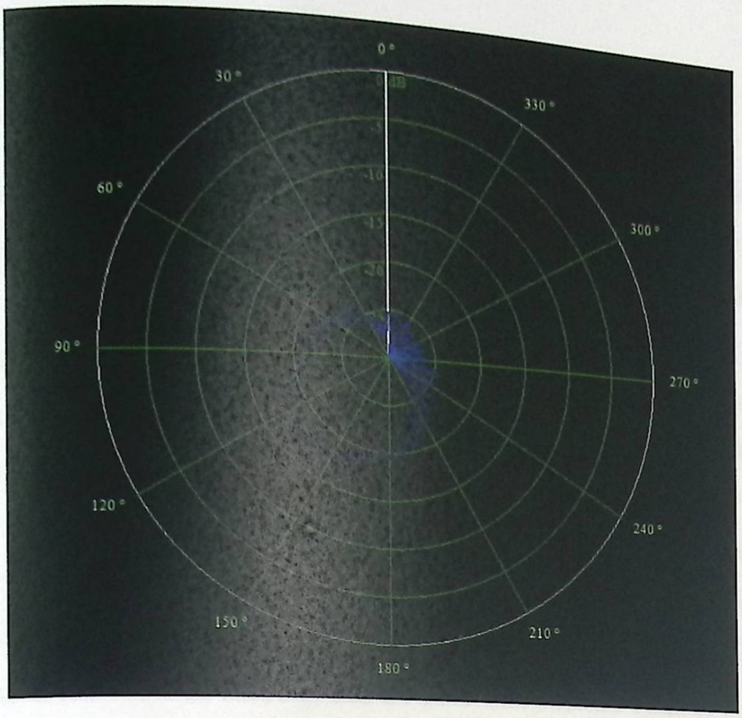

Figure 5.2.20: Measured H-plane radiation pattern of optimum antenna with normal skin on Rx only.

5.3 Conclusion

In conclusion, the return loss simulations and measurements show very close resemblance in terms of resonance frequencies and their return loss values , for the four cases; optimum and central feeding structures (with and without) a skin layer tissue.

With regard to the radiation patterns, the situation is different, because the synthetic normal skin and tumor made from yellow corn flour and water for normal skin and glycerin mixed with Zinc oxide for the cancer tumor tissue, did not exactly mimic the real parameters of the skin in terms of permittivity and conductivity at the selected frequency of resonance. The recipes were made within available possibilities and only the general experimental performance of the antennas in the various cases could be derived in terms of directivity and penetration loss. however, a good insight is derived from the simulated radiation patterns which conform with expectations. In other words, the optimum antenna with the skin gave a reference E-plane radiation pattern while with the added tumor layer, the penetration loss decreased while the gain increased since more surface current became available with the existence of a synthetic tumor, which in general has lower impedance than normal skin because of relatively higher permittivity and higher conductivity characteristics.

Education makes a people easy to lead, but difficult to drive, easy to govern but impossible to enslave.

Henry P. Brougham

6 Challenges and future work

6.1 Challenges

Rectangular microstrip antennas are widely used in many medical applications such as a microwave imaging and treatments.

Designing a microstrip antenna that have been compatible with skin to use it in breast cancer detection depends on the electrical properties for human skin specifically permittivity and conductivity.

A synthetic skin layer and tumor was simulated according to published papers by mixing a corn flour and water for skin and glycerin with zinc oxide for tumor. The confirmation of the electrical values for these two mixtures was not possible because we don't have a measurement devices that give the permittivity and conductivity values at 2.45 GHz.

6.2 Future work

The main feature for this microstrip antenna is its simplicity to get higher performance by using it with real human skin for experiments. This work can be leading to good detection for existing tumor and its location and give an accurate imaging result .

After that we can improved this to become a wearable antenna for easy and personal usage.

References

[16] S. S. Chaudhary, R. K. Mishra, A. Swarup, and J. M. Thomas, "Dielectric properties of normal and malignant human breast tissues at radiowave and microwave frequencies.," Indian J Biochem Biophys, vol. 21, pp. 76–79, Feb 1984.

[17] A. M. Campbell and D. V. Land, "Dielectric properties of female human breast tissue measured in vitro at 3.2 ghz.," Phys Med Biol, vol. 37, pp. 193–210, Jan 1992.

[18] W. T. Joines, Y. Zhang, C. Li, and R. L. Jirtle, "The measured electrical properties of normal and malignant human tissues from 50 to 900 mhz.," Med Phys, vol. 21, pp. 547–550, Apr 1994.

[19] M. Lazebnik, C. B. Watkins, S. C. Hagness, J. H. Booske, D. Popovic, L. Mc Cartney, M. Okoniewski, M. J. Lindstrom, T. M. Breslin, J. Harter, S. Sewall, W. Temple, D. Mew, A. Magliocco, and T. Ogilvie, "The dielectric properties of normal and malignant breast tissue at microwave frequencies: analysis, conclutions, and implications from the wisconsin/calgary study," in Proc. IEEE Antennas and Propagation International Symposium, pp. 2172–2175, 9–15 June 2007.

[20] X. Li, E. Bond, B. Van Veen, and S. Hagness, "An overview of ultra-wideband microwave imaging via space-time beamforming for early-stage breast-cancer detection," Antennas and Propagation Magazine, IEEE, vol. 47, pp. 19–34, Feb 2005.

[21] P. M. Meaney, Q. Fang, T. Rubaek, E. Demidenko, and K. D. Paulsen, "Log transformation benefits parameter estimation in microwave tomographic imaging.," Med Phys, vol. 34, pp. 2014–2023, Jun 2007.

[22] Kumar, G and Ray, K.P; "Broadband Microstrip Antenna", Artech House, 2003.

[23] C.A. Balanis, "Antenna theory: analysis and design," Third Editition, John Wiley 2005.

[24] I.J. Bahl and D.K. Trivedi, "A designer's guide to microstrip line," microwaves, pp.174-182, May 1977.

[25] Wafa sami, Sahar, Ahmed amro , "Design and Fabrication of Microstrip Tools for Measurement of Gain and Circularly Polarized Radiation Pattern",2013.

[1] R.Garg, P.Bhartia, I.Bahl and A.Ittipiboor, "Microstrip antenna design handbook, "Artech house, 2001.

[2] Dr.A.Mandal "History of Breast Cancer", Available at http://www.news-medical.net/health/History-of-Breast-Cancer.aspx .

[3] K. Planche and S. Vinnicombe, "Breast imaging in the new era," Cancer Imaging, vol. . 4, pp. 39–50, 2004.

[4]E. Alanen and I. V. Lindell, "Effect of skin in microwave detection of breast cancer," IEEE Transactions on Microwave Theory and Techniques, vol. 34, no. 5, pp. 584–588, 1986.

[5] S. Shrestha, M. Agarwal, P. Ghane, and K. Varahramyan, "Flexible Microstrip Antenna for Skin Contact Application", Vol. 2012, 4 June 2012.

[6]Ansoft HFSS, Ver. 12, Ansys Inc, http://www.ansys.com/.

[7] John P. Stang, "A 3D Active Microwave Imaging System for Breast Cancer Screening", Ph.D diss., Duke University, pp.1-2, 2008.

[8] Christine M. Nicola, " Circular Disk Microstrip Antenna For Wireless Communication", October 6 University, 2006 -2007.

[9] P. J. Lynch and C. C. Jaffe, "Breast Normal Anatomy Cross-section". Yale university Center for Advanced Instructional Media, 2007.

[10] D. B. Kopans, Breast Imaging. Lippincott Williams and Wilkins, 2007.

[11] L. E. Hughes, R. E. Mansel, and D. Webster, Benign Disorders and Diseases of the Breast. W. B. Saunders, 2000.

[12] J. H. Isaacs, Textbook of Breast Disease. Mosby, 1992

[13] Y. Hirshaut and P. I. Pressman, Breast Cancer: The Complete Guide. Bantam, 2000.

[14] W. T. Joines, R. L. Jirtle, M. D. Rafal, and D. J. Schaefer, "Microwave power absorption differences between normal and malignant tissue.," Int J Radiat Oncol Biol Phys, vol. 6, pp. 681–687, Jun 1980.

[15] W. T. Joines, S. Shrivastav, and R. L. Jirtle, "A comparison using tissue electrical properties and temperature rise to determine relative absorption of microwave power in malignant tissue.," Med Phys, vol. 16, no. 6, pp. 840–844, 1989.

[16] S. S. Chaudhary, R. K. Mishra, A. Swarup, and J. M. Thomas, "Dielectric properties of normal and malignant human breast tissues at radiowave and microwave frequencies.," Indian J Biochem Biophys, vol. 21, pp. 76–79, Feb 1984.

[17] A. M. Campbell and D. V. Land, "Dielectric properties of female human breast tissue measured in vitro at 3.2 ghz.," Phys Med Biol, vol. 37, pp. 193–210, Jan 1992.

[18] W. T. Joines, Y. Zhang, C. Li, and R. L. Jirtle, "The measured electrical properties of normal and malignant human tissues from 50 to 900 mhz.," Med Phys, vol. 21, pp. 547–550, Apr 1994.

[19] M. Lazebnik, C. B. Watkins, S. C. Hagness, J. H. Booske, D. Popovic, L. Mc Cartney, M. Okoniewski, M. J. Lindstrom, T. M. Breslin, J. Harter, S. Sewall, W. Temple, D. Mew, A. Magliocco, and T. Ogilvie, "The dielectric properties of normal and malignant breast tissue at microwave frequencies: analysis, conclutions, and implications from the wisconsin/calgary study," in Proc. IEEE Antennas and Propagation International Symposium, pp. 2172–2175, 9–15 June 2007.

[20] X. Li, E. Bond, B. Van Veen, and S. Hagness, "An overview of ultra-wideband microwave imaging via space-time beamforming for early-stage breast-cancer detection," Antennas and Propagation Magazine, IEEE, vol. 47, pp. 19–34, Feb 2005.

[21] P. M. Meaney, Q. Fang, T. Rubaek, E. Demidenko, and K. D. Paulsen, "Log transformation benefits parameter estimation in microwave tomographic imaging.," Med Phys, vol. 34, pp. 2014–2023, Jun 2007.

[22] Kumar, G and Ray, K.P; "Broadband Microstrip Antenna", Artech House, 2003.

[23] C.A. Balanis, "Antenna theory: analysis and design," Third Editition, John Wiley 2005.

[24] I.J. Bahl and D.K. Trivedi, "A designer's guide to microstrip line," microwaves, pp.174-182, May 1977.

[25] Wafa sami, Sahar, Ahmed amro , "Design and Fabrication of Microstrip Tools for Measurement of Gain and Circularly Polarized Radiation Pattern",2013.